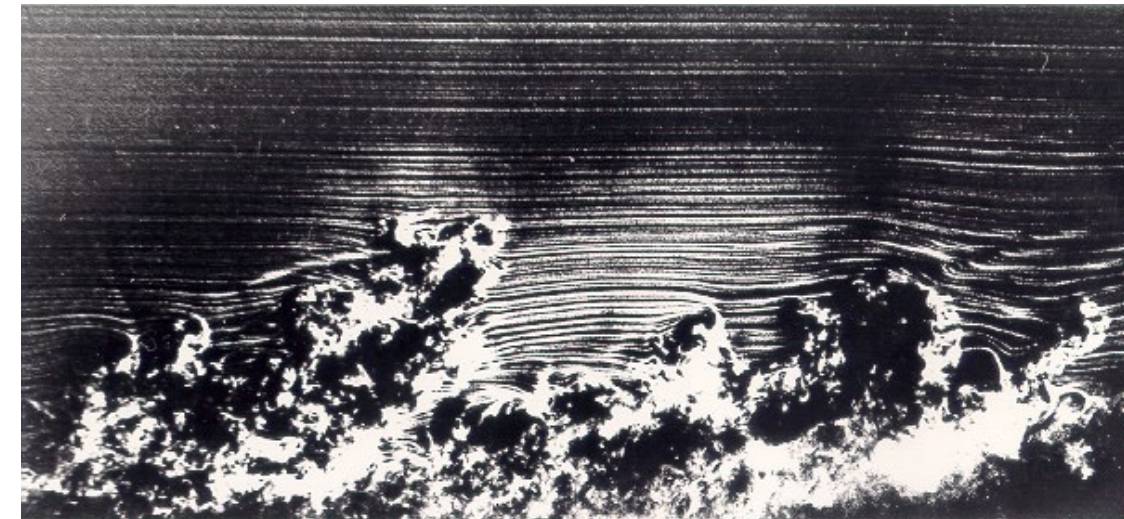


# ***A New Universal Velocity Profile for Wall Bounded Flows; Rapid calculation of airfoil viscous drag***

*Frank J. Malina Lecture*

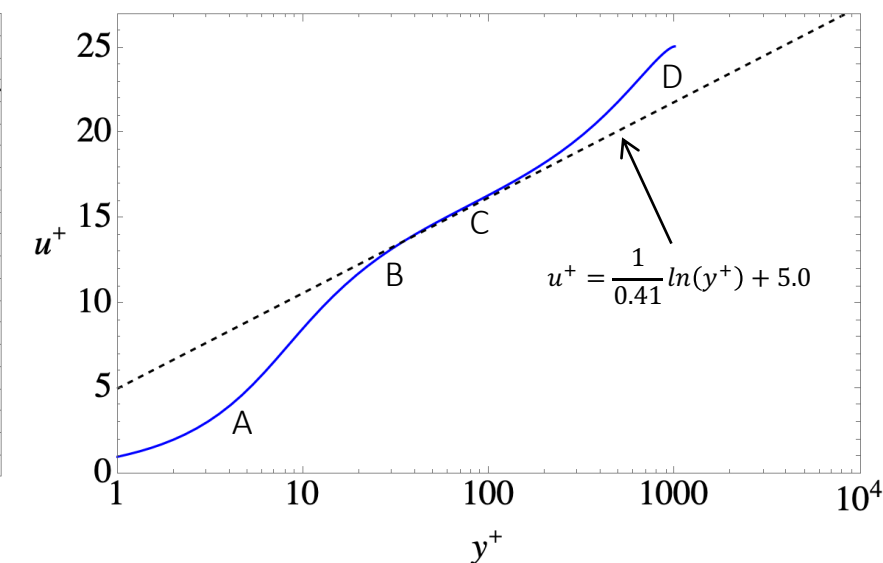
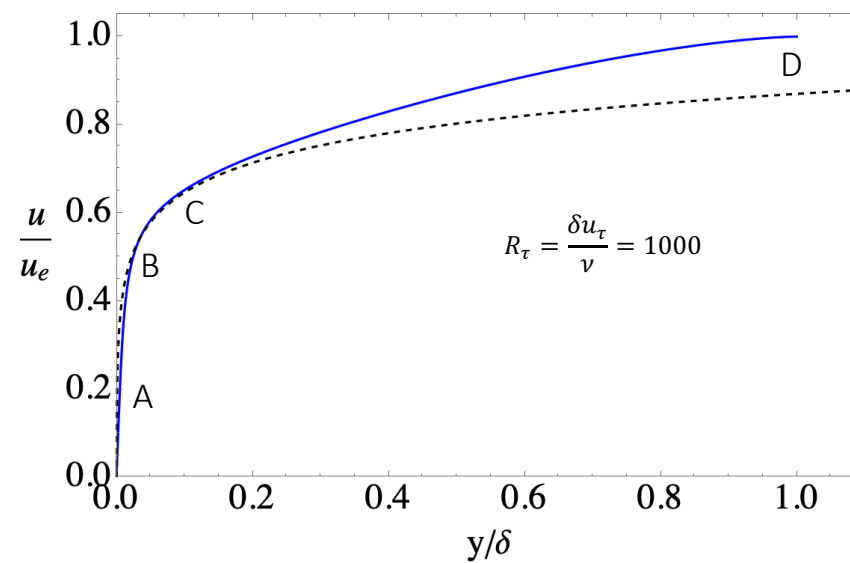
*Brian Cantwell  
Department of Aeronautics and Astronautics  
Stanford University*

## The turbulent boundary layer velocity profile



Van Dyke, Album of Fluid Motion, image 157. Smoke wire image by Corke, Guezennec and Nagib.

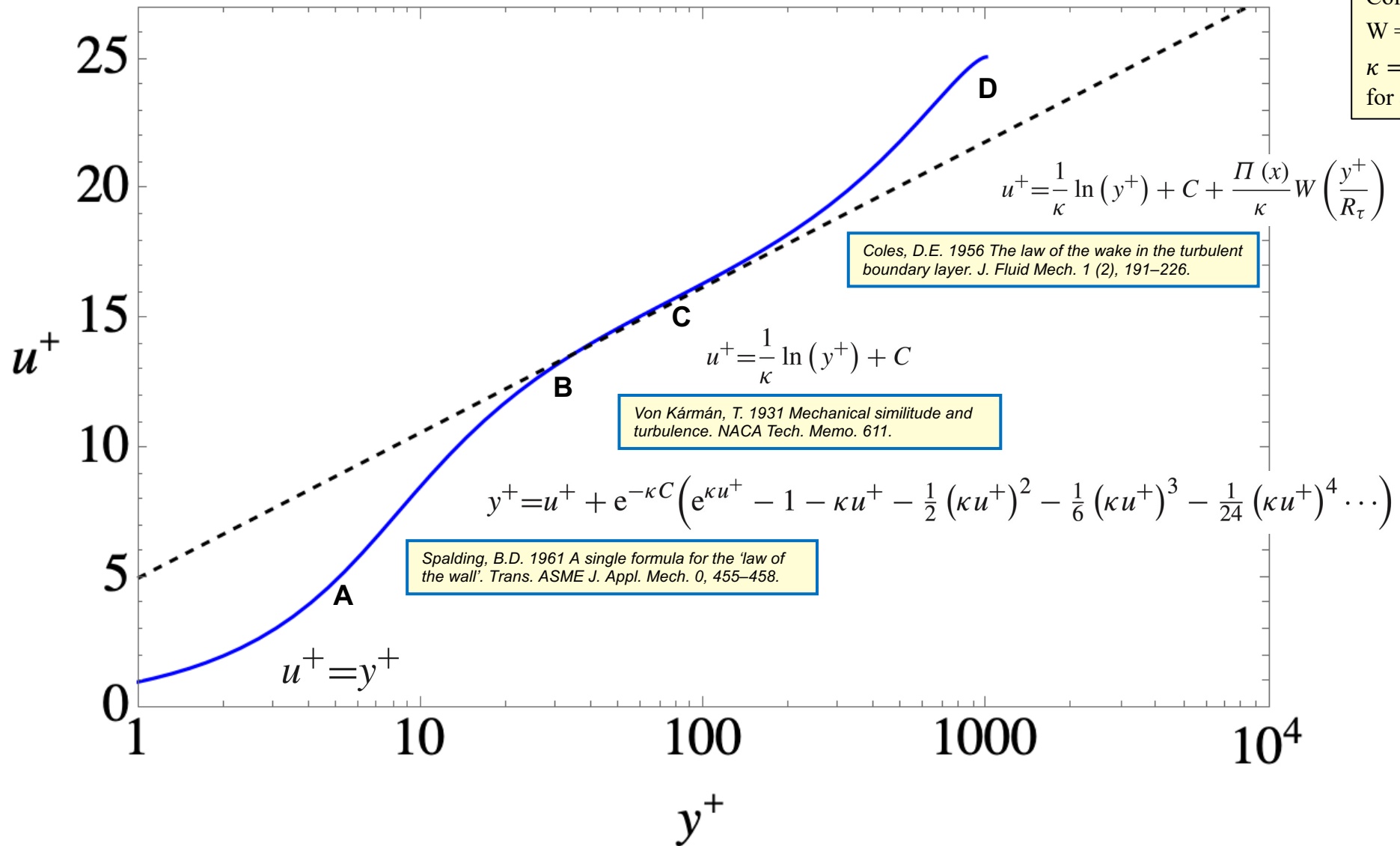
$$u_\tau = \sqrt{\frac{\tau_w}{\rho}} \quad \tau_w = \mu \frac{\partial U}{\partial y} \Big|_{y=0}$$



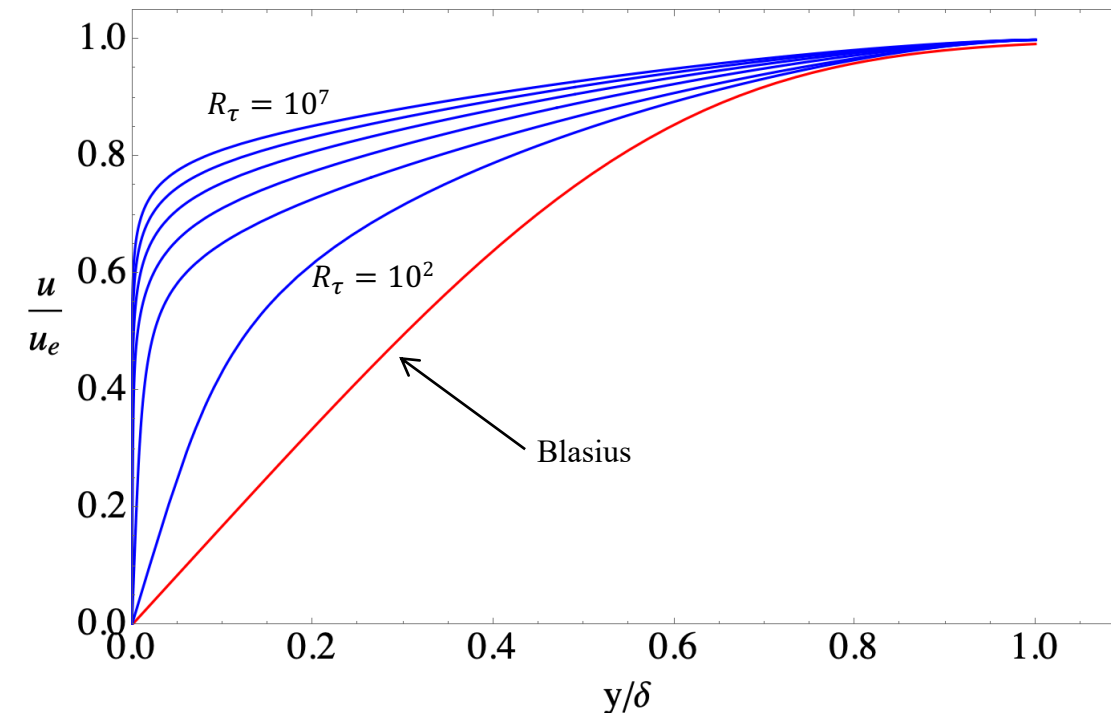
$$y^+ = \frac{yu_\tau}{\nu} \quad u^+ = \frac{u}{u_\tau}$$

$$R_\tau = \frac{\delta u_\tau}{\nu} = \delta^+$$

## Classical wall-wake formulation



## Reynolds number dependence of the velocity profile



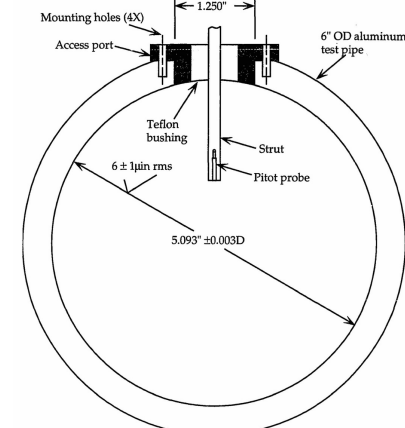
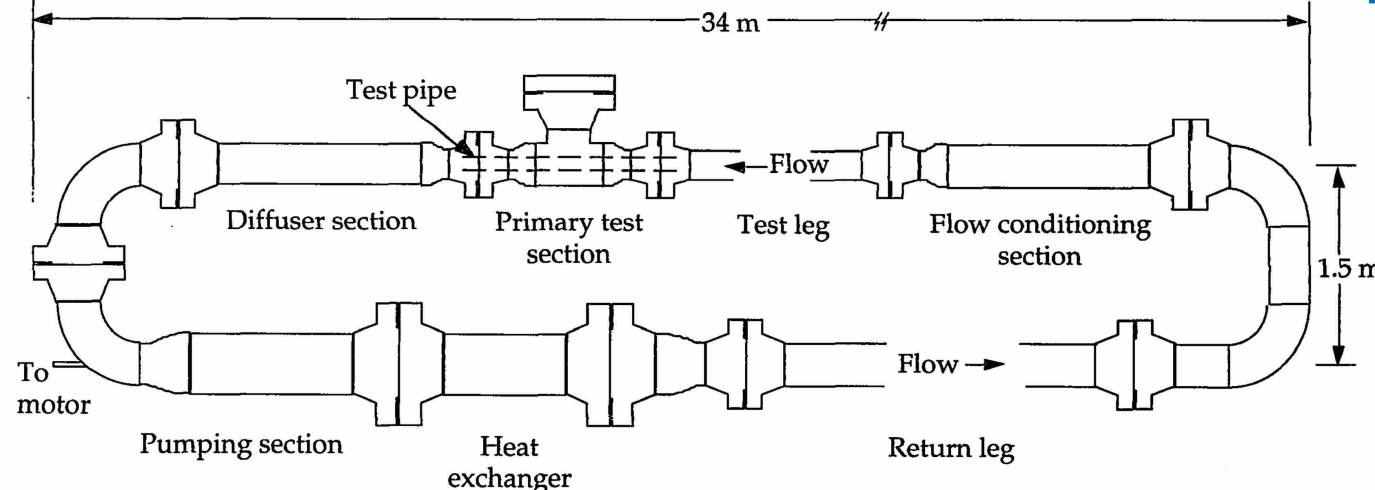
The thickness  $\delta$  is arbitrarily defined.  
Typically  $\delta_{0.99}$  or  $\delta_{0.995}$  is used  
where  
 $u(\delta)=0.99u_e$  or  $u(\delta)=0.995 u_e$ .

## Problems with the wall-wake profile

- 1) Separate layers need to be matched
- 2) Discontinuity in  $du/dy$  at the outer edge of the boundary layer due to the  $\ln(y^+)$  term
- 3) Profile is not connected to any model of the turbulent shear stress
- 4) The profile is inaccurate at low Reynolds numbers
- 5) No information as to the Reynolds number at which the profile applies

## The Princeton Superpipe (PSP) Facility

Zagarola, M. V. & Smits, A. J. 1998 Mean-flow scaling of turbulent pipe flow. *J. Fluid Mech.* 373, 33–79.



ZAGAROLA, M. V. 1996 Mean-flow scaling of turbulent pipe flow. Doctoral Dissertation, Princeton University.

Pitot tube diameter = 0.9mm

MCKEON, B. J. 2003 High Reynolds number turbulent pipe flow. Doctoral Dissertation, Princeton University.

Pitot tube diameter = 0.3mm

26 cases

$$19639 < R_e < 20,088,000$$

$$851 < R_\tau < 530,000$$

$$23 < u_0/u_\tau < 38$$

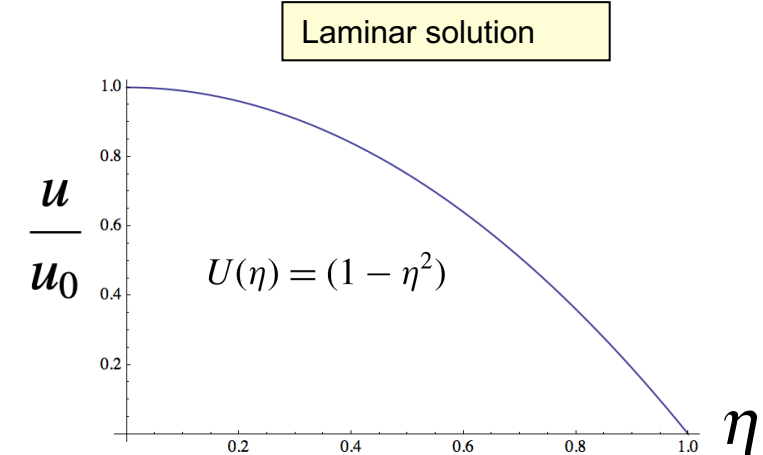
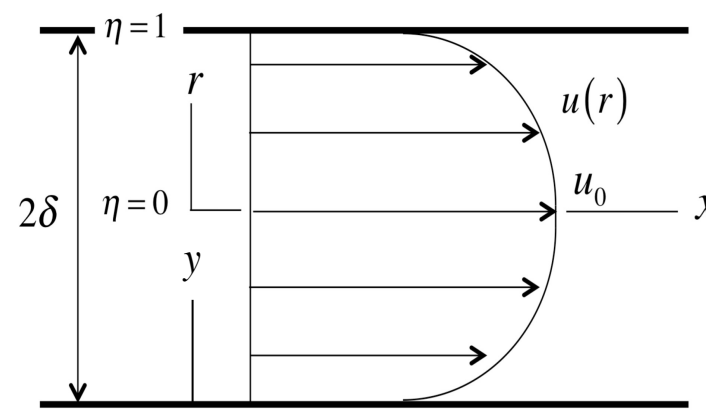
$$R_e = \frac{u_0 R}{\nu}$$

## Pipe Flow

$$\eta = \frac{r}{\delta}$$

$$U = \frac{u}{u_0}$$

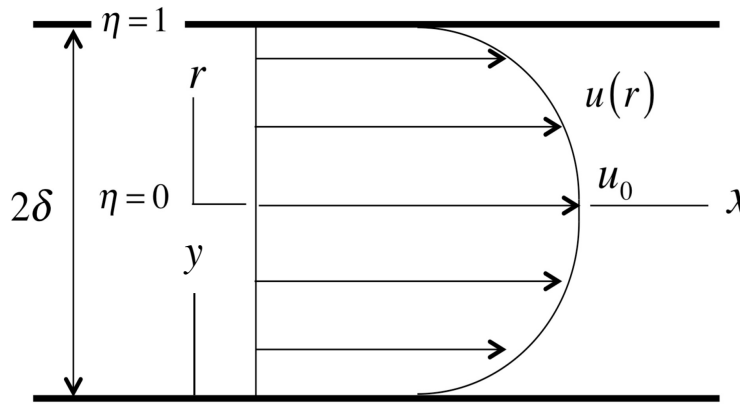
$$R_e = \frac{u_0 \delta}{\nu}$$



Balance between shear stress and the pressure gradient

$$\frac{1}{r} \frac{d}{dr} (r(\bar{u}'\bar{v}')) - \nu \frac{1}{r} \frac{d}{dr} \left( r \frac{du}{dr} \right) + \frac{1}{\rho} \frac{\partial p(x, r)}{\partial x} = 0$$

## Pipe Flow – wall variables



Laminar solution in wall variables

$$u_{laminar}^+ = y^+ \left( 1 - \frac{y^+}{2R_\tau} \right)$$

$$C_{flaminar} = \frac{8}{R_\tau^2}$$

$$u_\tau = \left( -\frac{\tau_w}{\rho} \right)^{1/2}$$

$$R_\tau = \frac{\delta u_\tau}{\nu}$$

Integrate the governing equation once and apply the centerline boundary condition  $dU/dr = 0$  at  $r = 0$ . Express the first order governing equation in terms of wall variables.

$$\tau^+ + \frac{du^+}{dy^+} - \left( 1 - \frac{y^+}{R_\tau} \right) = 0$$

$$u^+ = \frac{u}{u_\tau} \quad y^+ = \frac{yu_\tau}{\nu} \quad \tau^+ = \frac{\overline{u'v'}}{u_\tau^2}$$

Note

$$\frac{u_0}{u_\tau} \equiv \frac{R_e}{R_\tau} \equiv \sqrt{\frac{2}{C_f}}$$

## Mixing length model for the turbulent shear stress

$$\tau^+ = \left( \lambda(y^+) \frac{du^+}{dy^+} \right)^2$$

Prandtl 1934

The first order governing equation becomes a quadratic equation in the derivative of the mean velocity

$$\left( \frac{du^+}{dy^+} \right)^2 + \frac{1}{\lambda(y^+)^2} \frac{du^+}{dy^+} - \frac{1}{\lambda(y^+)^2} \left( 1 - \frac{y^+}{R_\tau} \right) = 0$$

Take the positive root

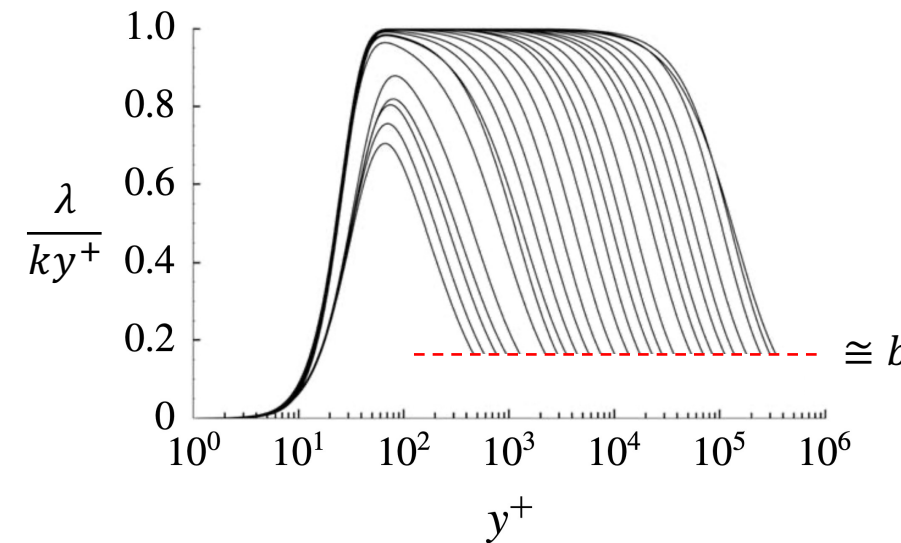
$$\frac{du^+}{dy^+} = -\frac{1}{2\lambda(y^+)^2} + \frac{1}{2\lambda(y^+)^2} \left( 1 + 4\lambda(y^+)^2 \left( 1 - \frac{y^+}{R_\tau} \right) \right)^{1/2}$$

Remove the singularity at  $\lambda = 0$

$$\frac{du^+}{dy^+} = \frac{2 \left( 1 - \frac{y^+}{R_\tau} \right)}{1 + \left( 1 + 4\lambda (y^+)^2 \left( 1 - \frac{y^+}{R_\tau} \right) \right)^{1/2}}$$

# Define a new mixing length function

$$\lambda(y^+) = \frac{ky^+(1 - e^{-(y^+/a)^m})}{\left(1 + \left(\frac{y^+}{bR_\tau}\right)^n\right)^{1/n}}$$



Cantwell, A universal velocity profile for smooth wall pipe flow, JFM vol 878, 2019

*k* - essentially the Karman constant.

*a* - wall damping length scale similar to the van Driest length.

*m* - exponent that, along with *a*, governs the shape and thickness of the near wall profile.

*b* - length scale proportional to the distance above the wall of the beginning of the outer layer.

*n* - exponent that, along with *b*, controls the transition of the profile to the wake function.

Later we will see that, for boundary layers, *b* and *n* can be related through a modified Clauser parameter  $\beta_c$ .

# The Universal Velocity Profile (UVP)

Integrate the velocity derivative from the wall

$$u^+(k, a, m, b, n, R_\tau, y^+) = \int_0^{y^+} \frac{2\left(1 - \frac{s}{R_\tau}\right)}{1 + \left(1 + 4\lambda^2\left(1 - \frac{s}{R_\tau}\right)\right)^{1/2}} ds$$

The velocity profile is uniformly valid from the wall to the pipe centerline at all Reynolds numbers.

$$\lambda(y^+) = \frac{ky^+(1 - e^{-(y^+/a)^m})}{\left(1 + \left(\frac{y^+}{bR_\tau}\right)^n\right)^{1/n}}$$

The velocity profile reduces to the laminar solution in the limit of zero Reynolds number independent of the choice of  $\lambda$ .

$$\lim_{R_\tau \rightarrow 0} \int_0^{y^+} \frac{2\left(1 - \frac{s}{R_\tau}\right)}{1 + \left(1 + 4\lambda^2\left(1 - \frac{s}{R_\tau}\right)\right)^{1/2}} ds = y^+ \left(1 - \frac{y^+}{2R_\tau}\right)$$

$$\lim_{R_\tau \rightarrow 0} C_f = \frac{2}{\left(\lim_{R_\tau \rightarrow 0} \int_0^{R_\tau} \frac{2\left(1 - \frac{s}{R_\tau}\right)}{1 + \left(1 + 4\lambda^2\left(1 - \frac{s}{R_\tau}\right)\right)^{1/2}} ds\right)^2} = \frac{8}{R_\tau^2}$$

# Determination of best fit model parameters

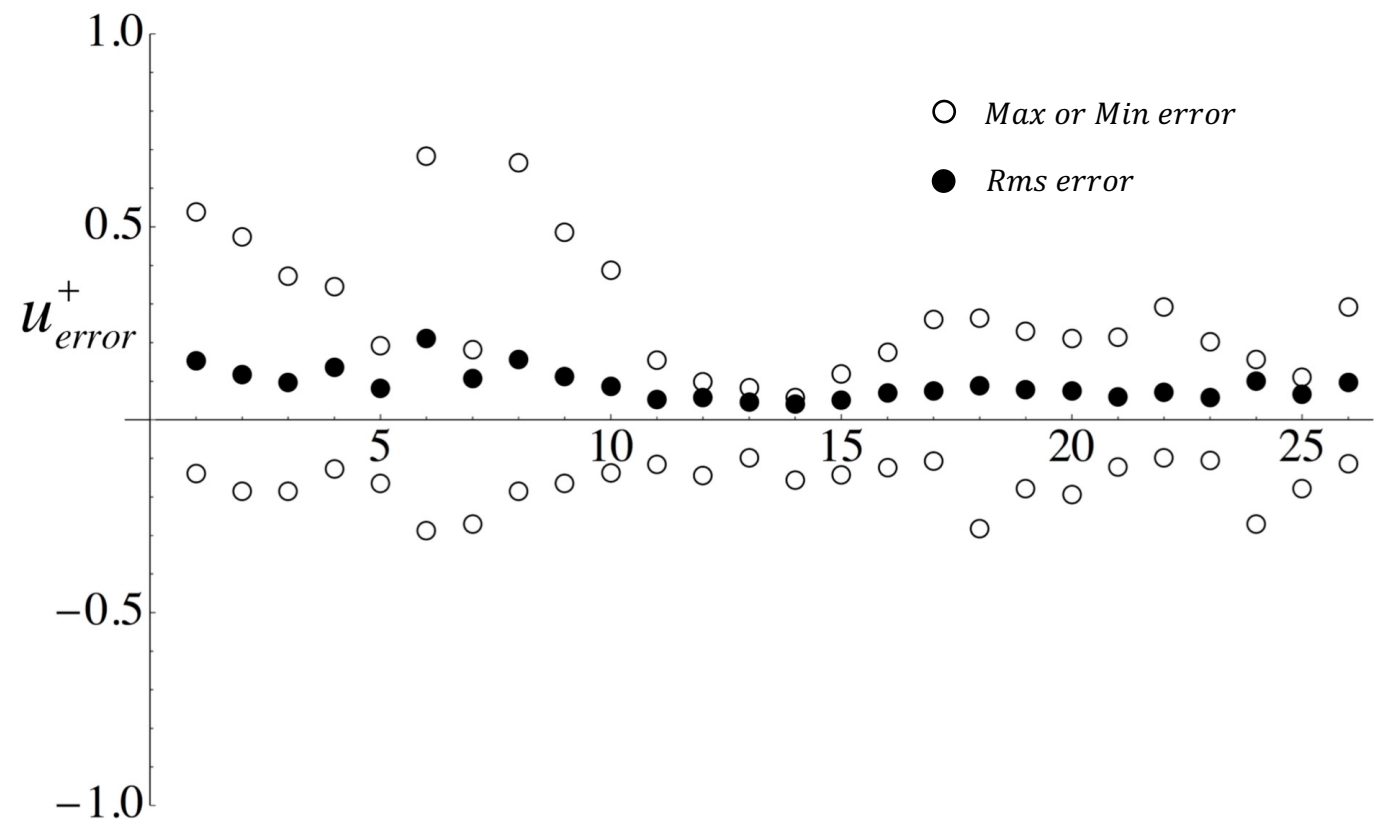
Minimize G with respect to k, a, m, b, n

$$G = \sum_{i=1}^N (u^+(k, a, m, b, n, y_i^+) - u_i^+(y_i^+))^2$$

Flow conditions and optimal model parameters for all 26 velocity profiles

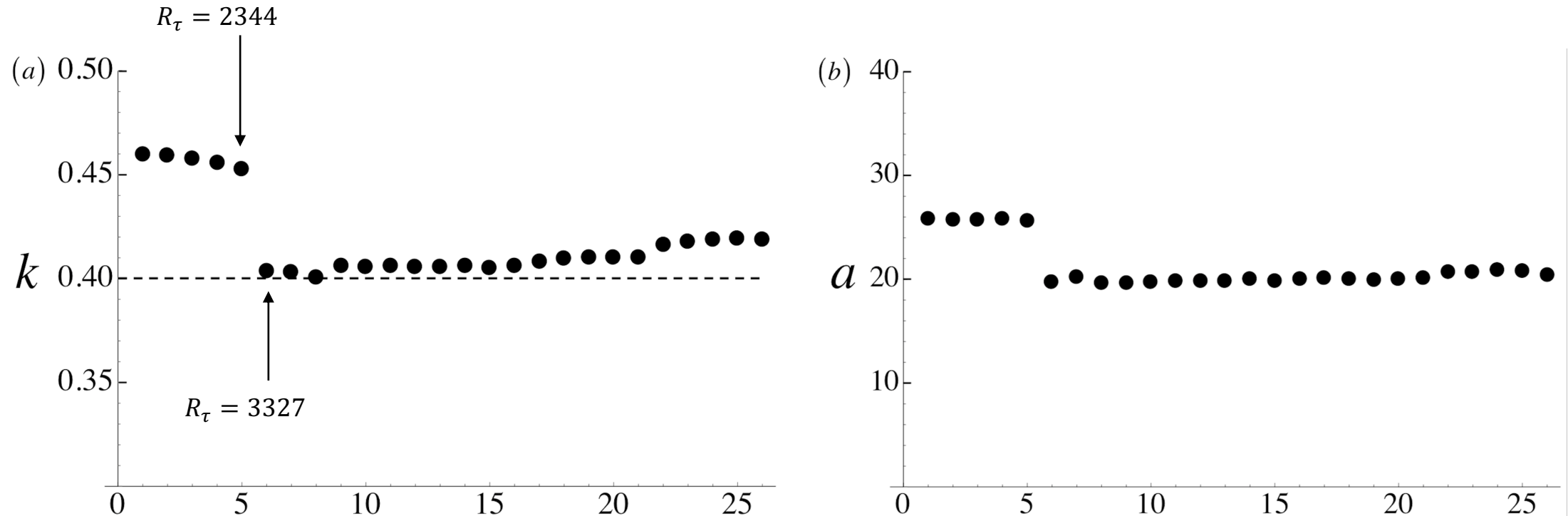
PSP #	$p_d$ mm	$u_\tau$	$R_\tau$	$R_e$	$\bar{R}_e$	$k$	$a$	$m$	$b$	$n$	$u_0 / u_\tau$	$u_{\text{rms error}}^+$	$u_{\text{max error}}^+$	$u_{\text{min error}}^+$
1	0.9	0.2089	850.947	19639.	15789.	0.459526	25.801	1.28798	0.299588	1.23686	23.0788	0.152301	0.538874	-0.139258
2	0.9	0.2683	1090.56	25818.	20864.	0.45944	25.7568	1.28759	0.293575	1.24395	23.6738	0.116743	0.474895	-0.185527
3	0.9	0.3455	1430.26	34818.	28339.	0.457774	25.7518	1.28734	0.291299	1.24498	24.3436	0.0971337	0.371735	-0.184978
4	0.3	0.432	1824.72	45284.	37173.	0.455477	25.863	1.25214	0.295422	1.18658	24.8171	0.135614	0.344811	-0.128301
5	0.9	0.5641	2344.74	59872.	49406.	0.452669	25.6633	1.29994	0.297001	1.2471	25.5345	0.0807474	0.192072	-0.164053
6	0.3	0.7919	3327.37	87150.	72290.	0.403394	19.7637	1.4964	0.350243	1.33343	26.1918	0.211454	0.682335	-0.287154
7	0.9	1.0065	4124.89	110550.	92715.	0.403106	20.2094	1.61048	0.341454	1.51165	26.8018	0.107034	0.182098	-0.270575
8	0.3	0.4183	5108.56	139380.	116990.	0.400524	19.6565	1.55346	0.353091	1.37315	27.284	0.155725	0.666555	-0.185794
9	0.3	0.5437	6617.44	183270.	154820.	0.406081	19.682	1.61578	0.330602	1.48471	27.6954	0.112958	0.485734	-0.164828
10	0.3	0.7035	8536.62	242050.	205430.	0.405547	19.7355	1.63359	0.32875	1.51099	28.3537	0.0863432	0.387908	-0.137764
11	0.3	0.9003	10914.4	314810.	268470.	0.406278	19.8188	1.6433	0.322005	1.61863	28.8432	0.0533497	0.155367	-0.114963
12	0.3	0.2423	14848.9	439790.	376800.	0.405533	19.8187	1.63899	0.317069	1.64829	29.6175	0.0582442	0.0984979	-0.144372
13	0.3	0.323	19778.3	599100.	515450.	0.405505	19.8541	1.64732	0.323093	1.66532	30.2907	0.0456737	0.0825095	-0.0989688
14	0.3	0.4136	25278.1	780760.	673100.	0.406013	19.9893	1.6426	0.317063	1.75114	30.8868	0.0411267	0.0582979	-0.156567
15	0.3	0.5411	32869.1	1038300.	897500.	0.40532	19.8023	1.65305	0.32421	1.66428	31.5881	0.0508534	0.118501	-0.14304
16	0.3	0.7001	42293.5	1363000.	1181500.	0.406164	19.9961	1.62818	0.307786	1.71916	32.2268	0.0690966	0.175211	-0.12347
17	0.3	0.4721	54530.6	1785500.	1552500.	0.407998	20.075	1.6311	0.30966	1.73322	32.743	0.0743128	0.259387	-0.106957
18	0.3	0.1759	76479.8	2558700.	2231100.	0.40993	20.0117	1.65763	0.326951	1.68545	33.4563	0.0885882	0.262977	-0.281911
19	0.3	0.2358	102200.	3500000.	3056400.	0.409934	19.9569	1.64637	0.317958	1.66433	34.2462	0.0779887	0.228758	-0.17882
20	0.3	0.2147	127914.	4457300.	3903100.	0.410112	20.0706	1.63716	0.312475	1.64664	34.8458	0.074515	0.211301	-0.192975
21	0.3	0.2782	165704.	5884200.	5157000.	0.410176	20.0915	1.64094	0.314927	1.6552	35.5102	0.0595818	0.214504	-0.122477
22	0.3	0.3652	216979.	7813500.	6859500.	0.416118	20.6722	1.58559	0.293151	1.68512	36.0106	0.0706957	0.292235	-0.0989045
23	0.3	0.4821	284254.	10392000.	9154000.	0.417539	20.673	1.59258	0.294283	1.67078	36.5586	0.058332	0.20287	-0.105169
24	0.9	0.6168	366972.	13540000.	11989000.	0.418696	20.8983	1.62571	0.306356	1.75128	36.8963	0.0999892	0.155755	-0.269669
25	0.9	0.7571	452380.	16888000.	14964000.	0.419289	20.8329	1.62031	0.303987	1.73244	37.3313	0.0669581	0.109743	-0.178982
26	0.3	0.9127	530023.	20088000.	17862000.	0.418993	20.3797	1.64264	0.314469	1.49687	37.9002	0.096876	0.291624	-0.114251

## Error



Average rms error  
= 0.096, ~ 0.3%

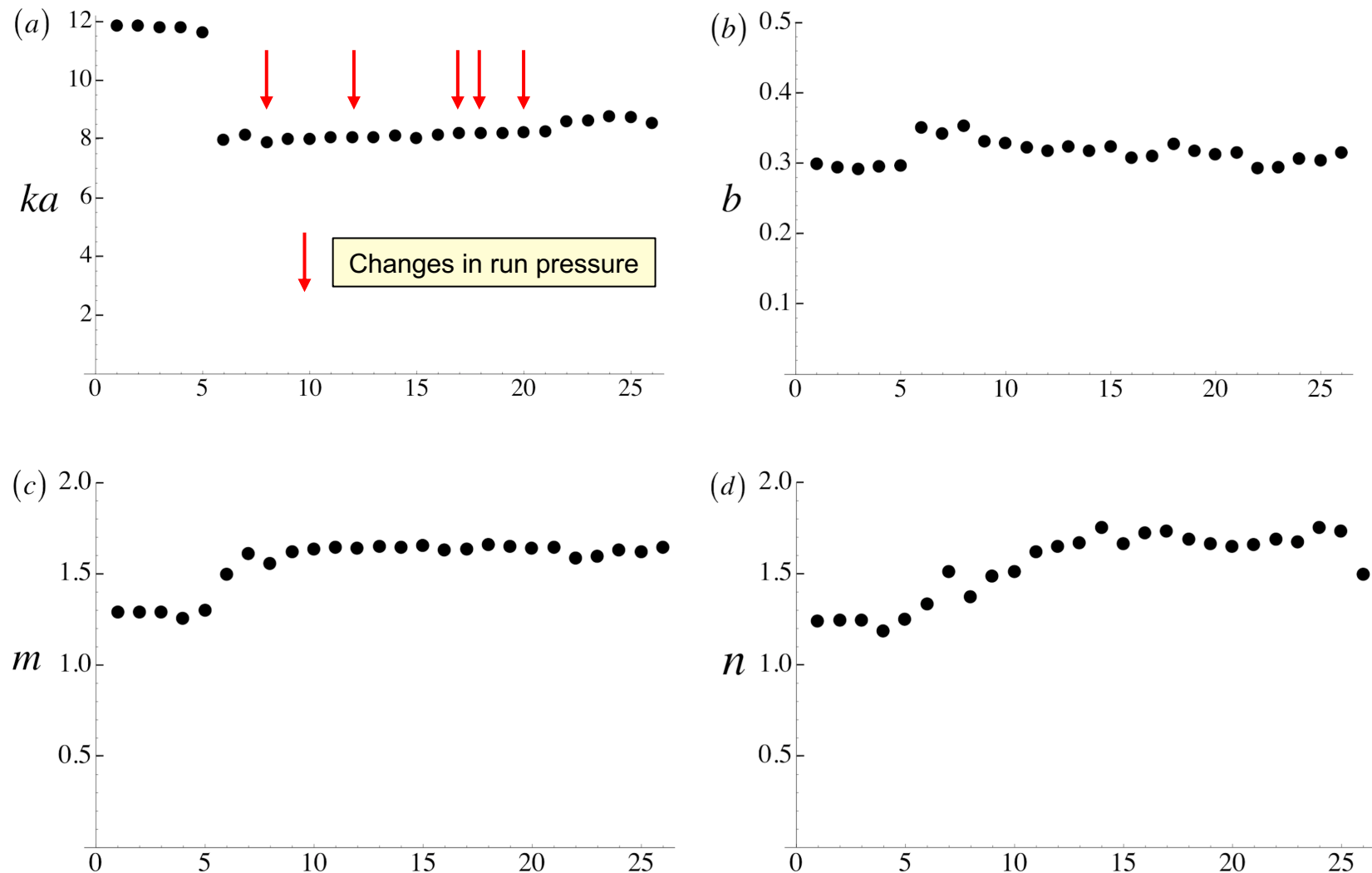
## Optimal values of k and a



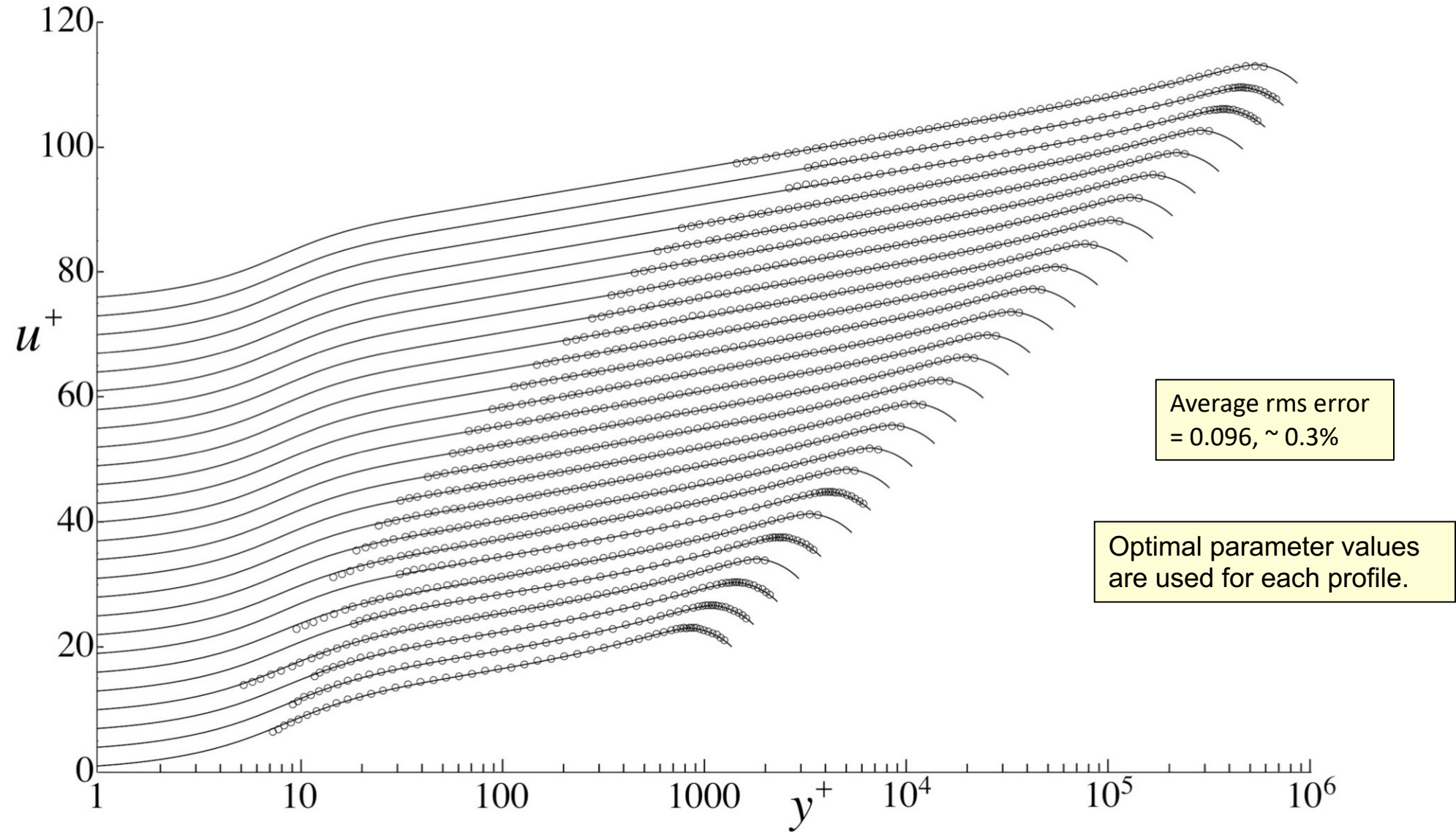
McKeon, B. J. & Morrison, J. F. 2007 Asymptotic scaling in turbulent pipe flow. *Phil. Trans. R. Soc.* 365, 771–787.

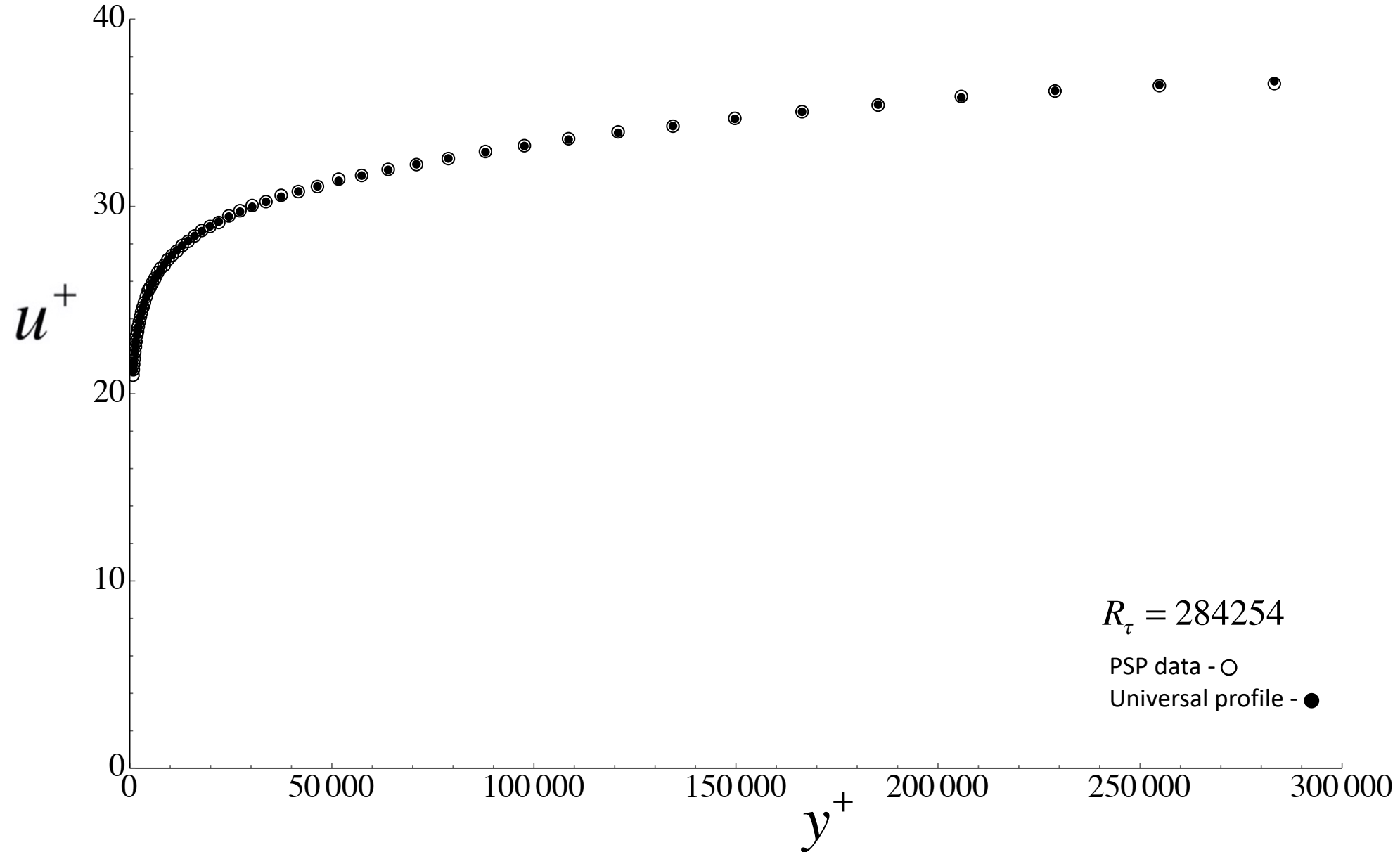
They note the absence of a logarithmic portion of the profile below  $R_\tau=5000$ , the beginning of scale separation and a possible "mixing transition" in pipe flow similar to that seen in free shear flow.

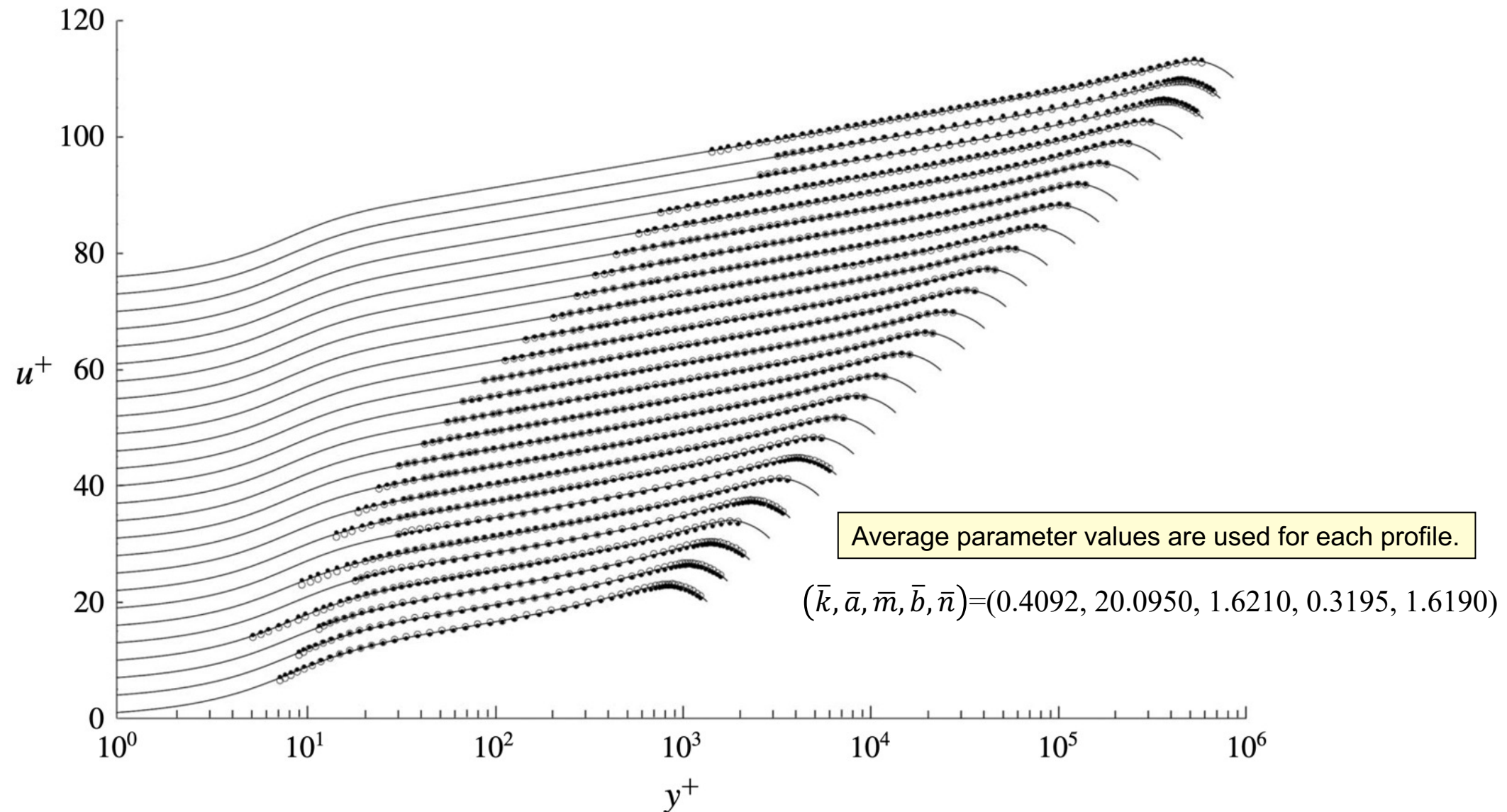
# Optimal values of $ka$ , $b$ , $m$ and $n$



## Comparison between PSP data and the universal velocity profile





PSP Smooth-wall Pipe Flow,  $R_\tau = 851$  to 530023

# Channel Flow

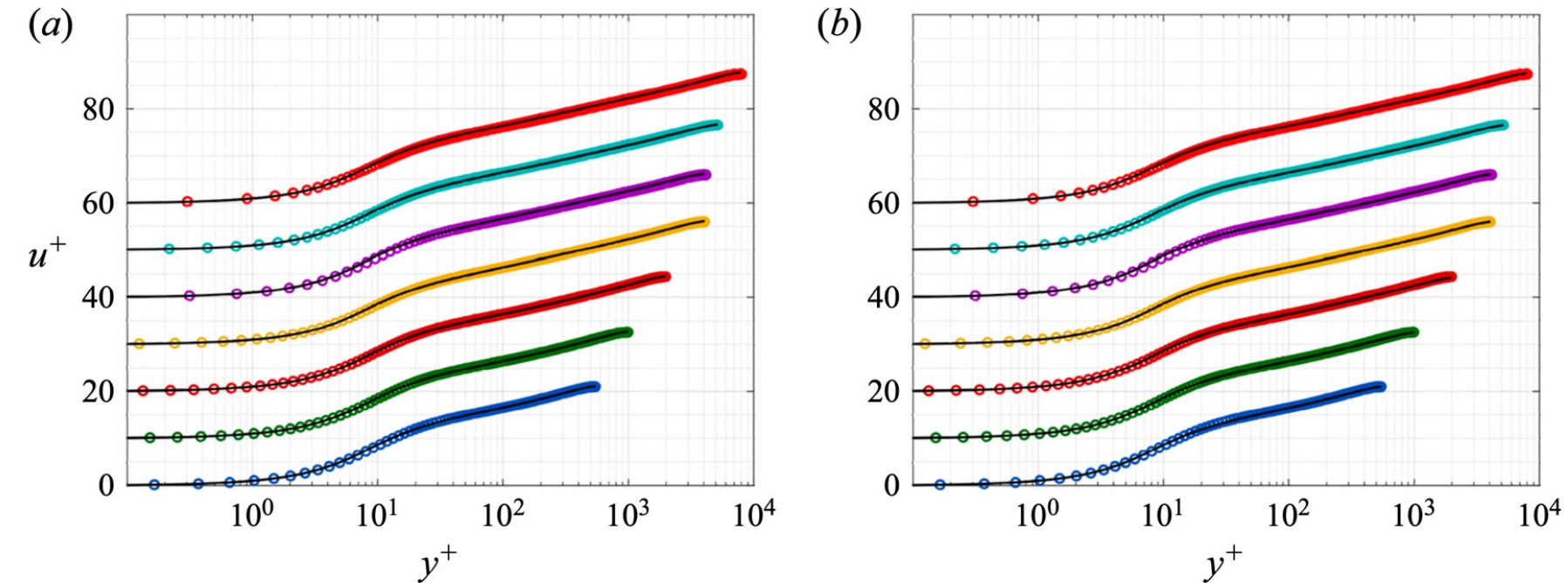
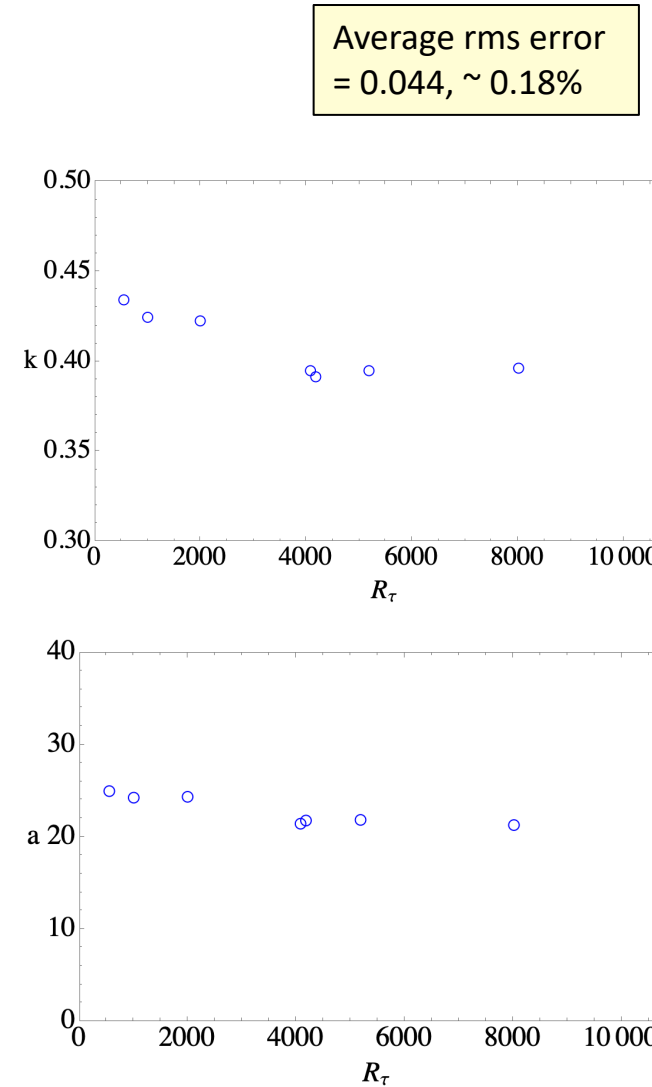
Channel Flow,  $R_\tau = 550$  to 8016

Figure 6. Channel flow velocity profiles from Lee & Moser (2015), Lozano-Durán & Jiménez (2014), Bernardini *et al.* (2014) and Yamamoto & Tsuji (2018) overlaid on the universal velocity profile with (a) optimal parameters from table 3 and (b) average parameter values from table 1 for  $(\bar{k}, \bar{a}, \bar{m}, \bar{b}, \bar{n})$  at  $R_\tau = 550$  (dark blue), 1001 (green), 1995 (dark red), 4079 (yellow), 4179 (purple), 5186 (light blue), 8016 (light red). Profiles are separated vertically by 10 units.

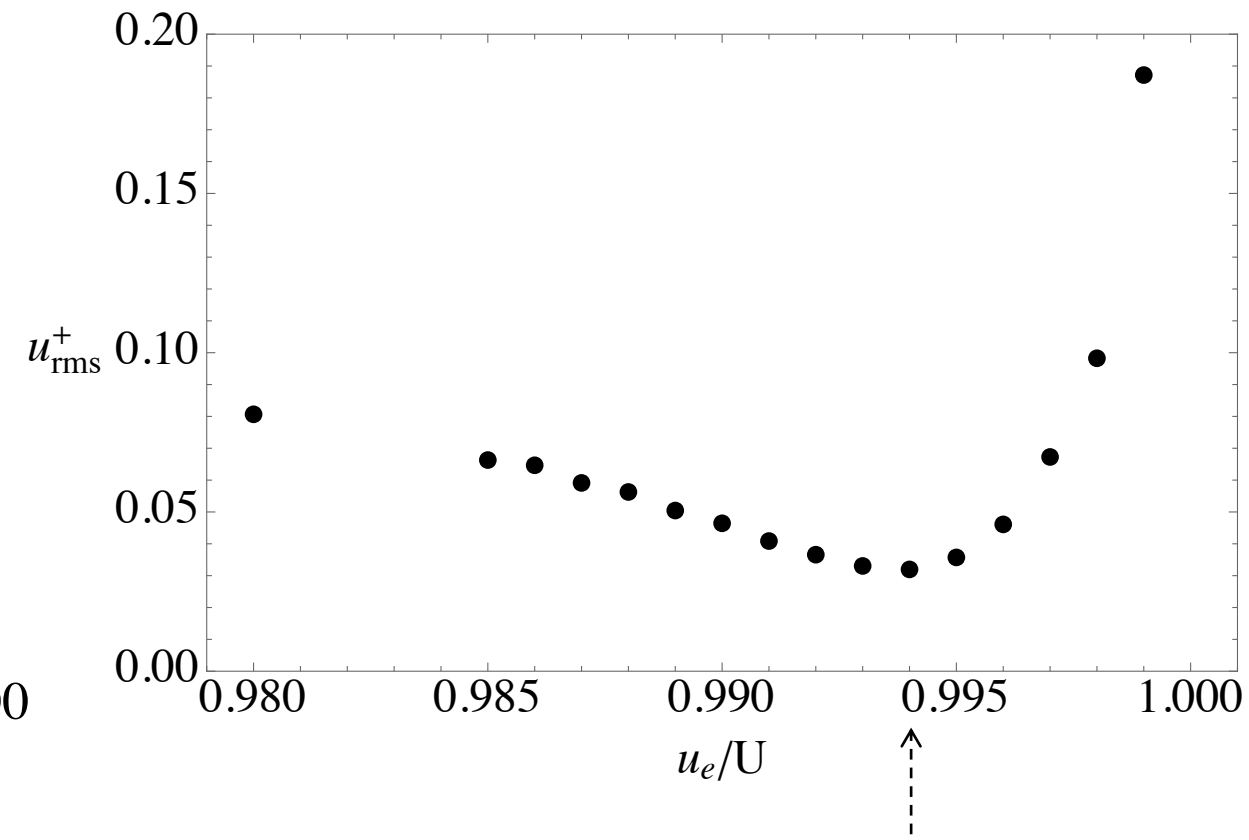
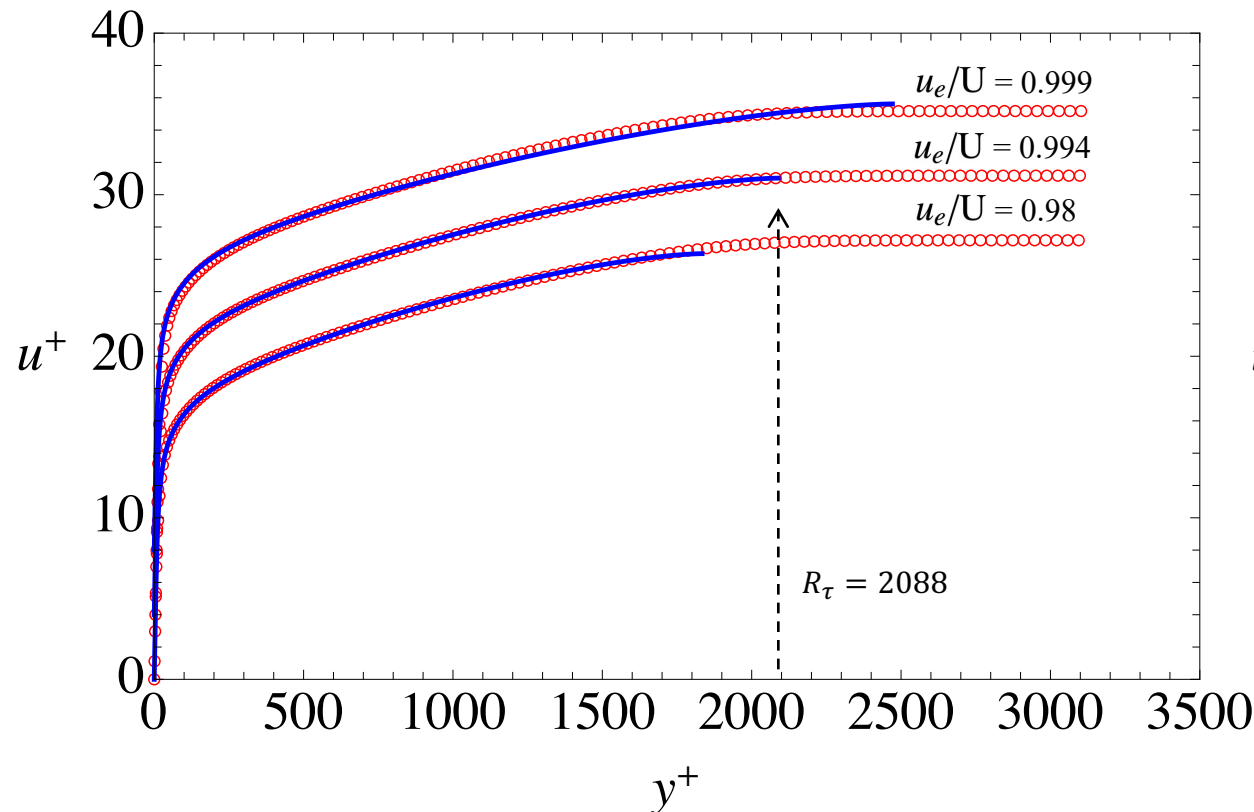
Average parameter values are used for each profile on the right.

$$(\bar{k}, \bar{a}, \bar{m}, \bar{b}, \bar{n}) = (0.4086, 22.8673, 1.2569, 0.4649, 1.3972)$$

## Zero Pressure Gradient Turbulent Boundary Layer

## Turbulent Boundary Layer equivalent channel half height (overall thickness)

$\delta_h$  is defined as the thickness that minimizes the error between a specific data set and the UVP



J. A. Sillero, J. Jimenez & R. D. Moser 2013 One-point statistics for turbulent wall-bounded flows at Reynolds numbers up to  $\delta^+ = 2000$ . *Phys. Fluids* 25 (10), 105102.

$\delta_h = \delta_{0.994}$

# ZPG Turbulent Boundary Layer Flow, $R_\tau = 1343$ to 2571

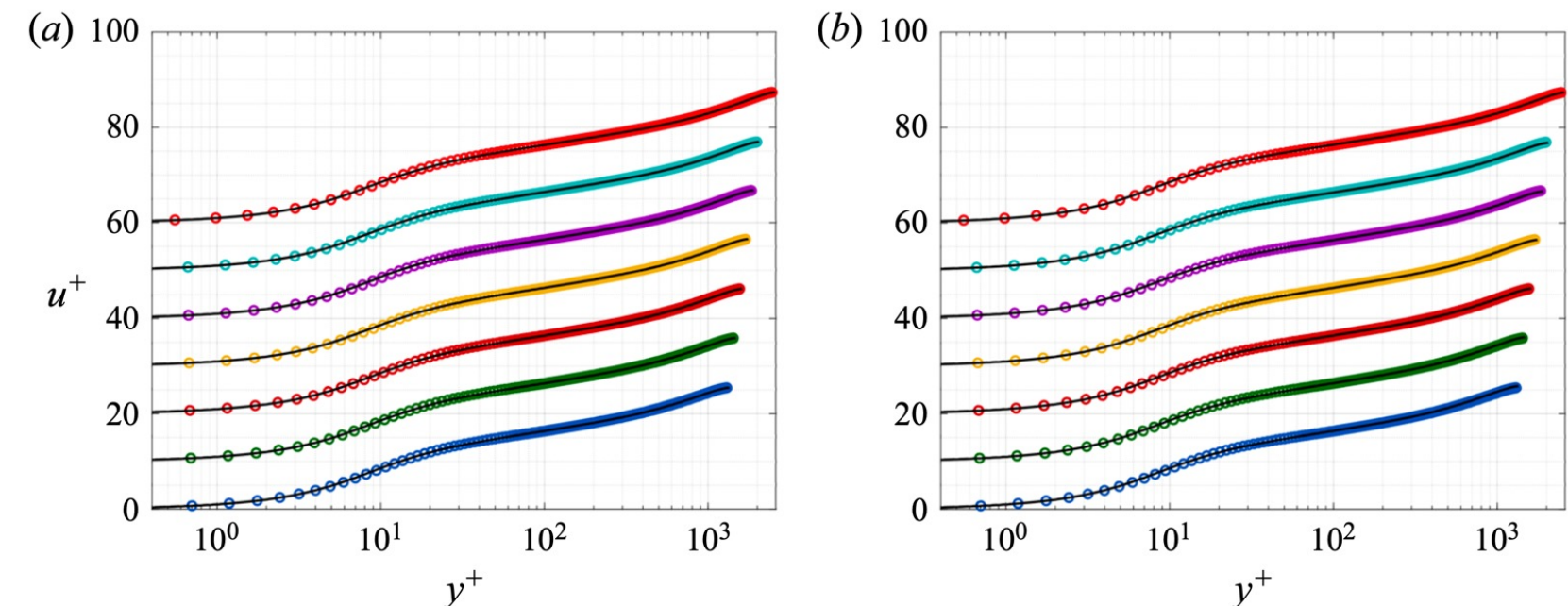
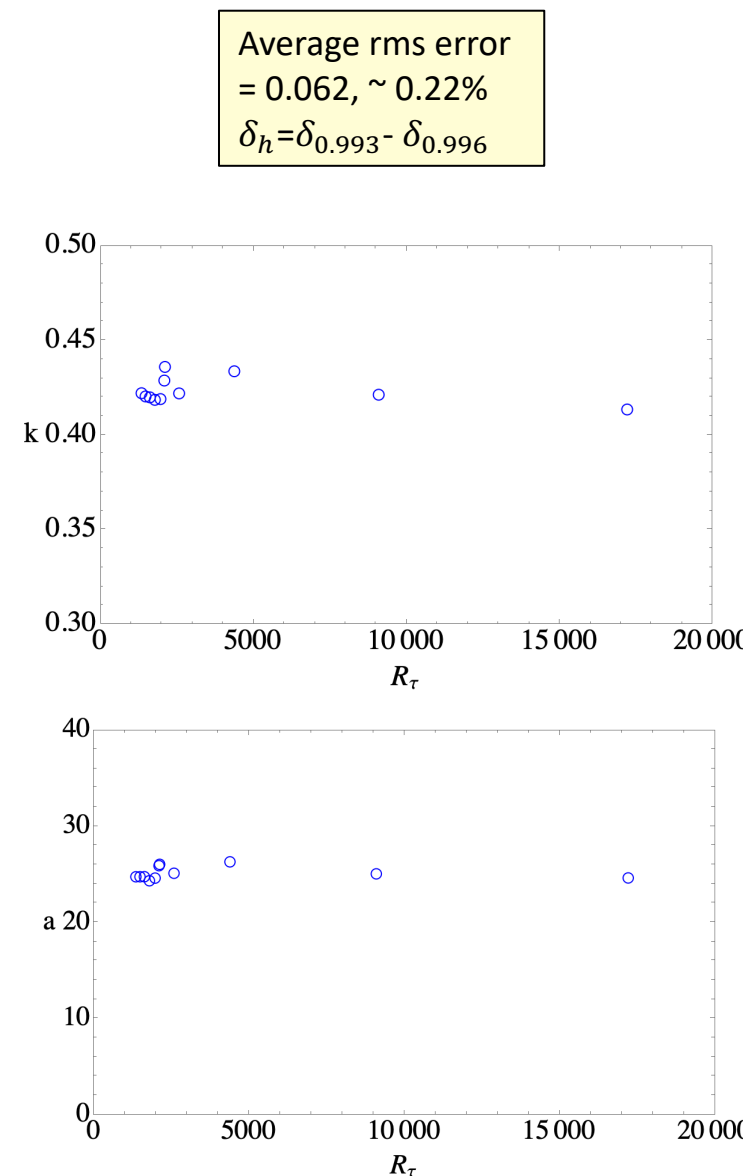
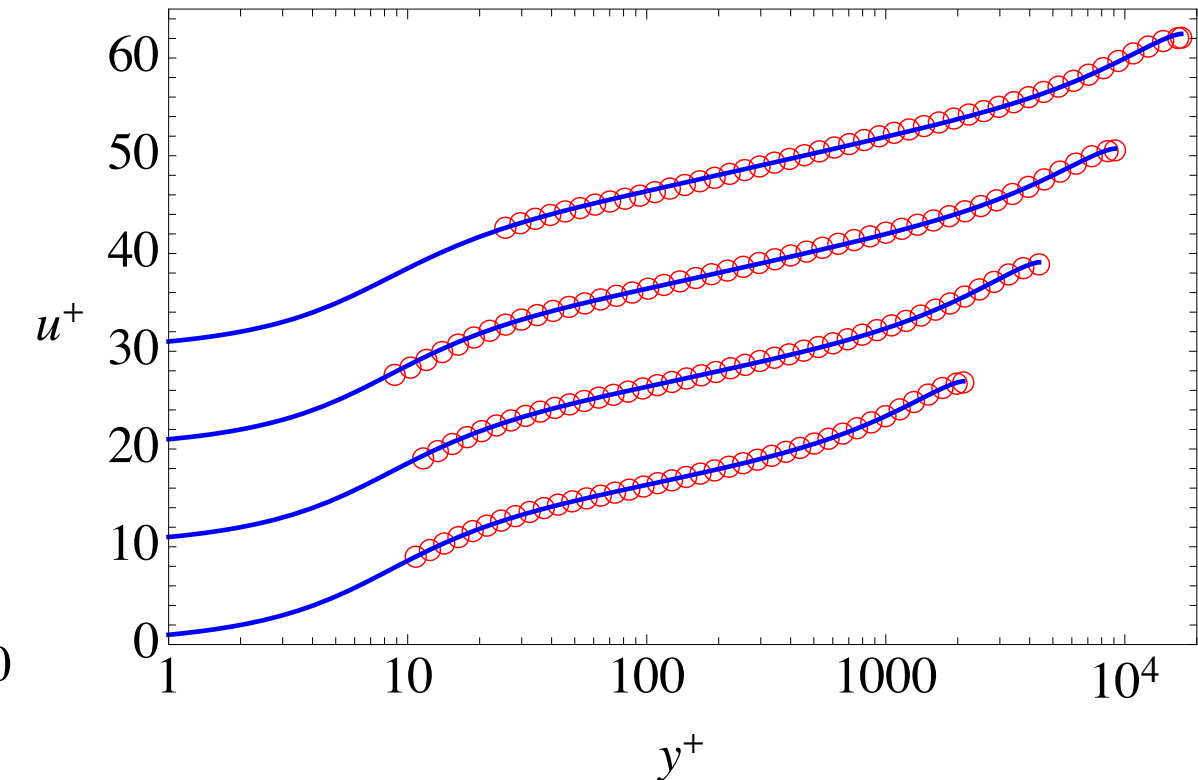
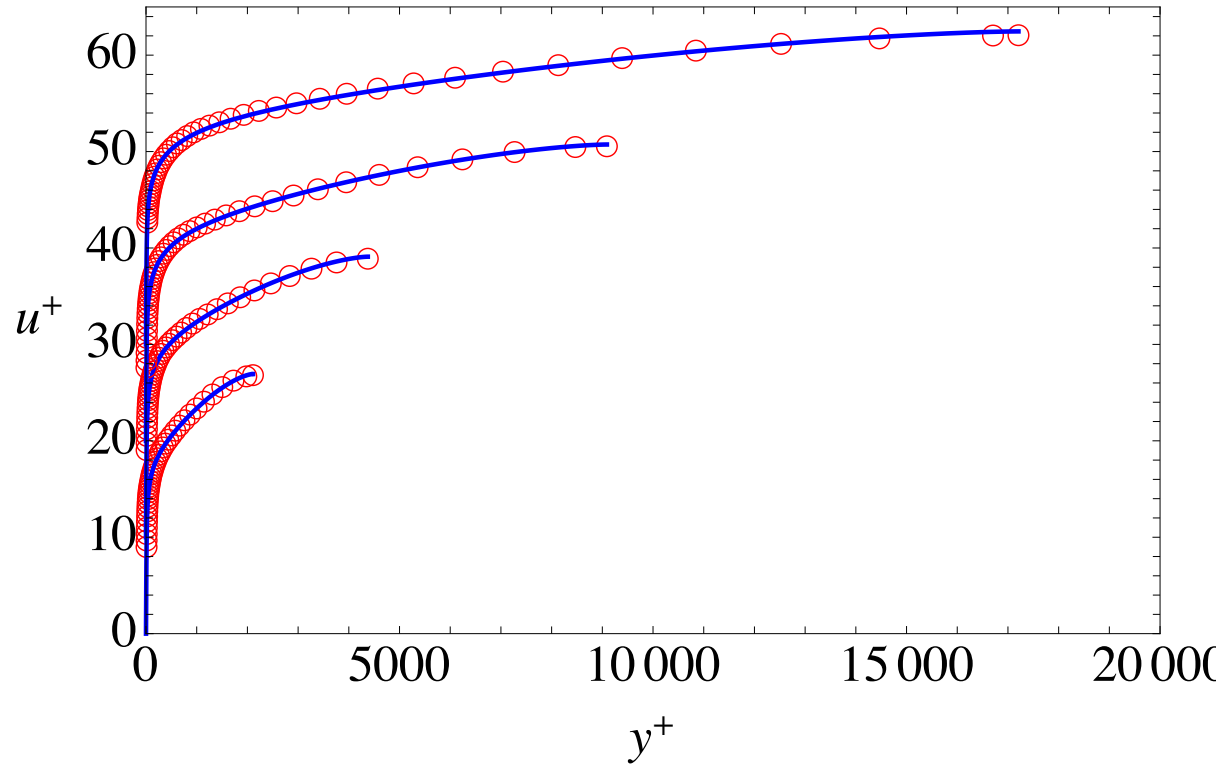


Figure 12. Turbulent boundary layer DNS data from Simens *et al.* (2009), Borrell *et al.* (2013), Sillero *et al.* (2013) and Eitel-Amor *et al.* (2014) at  $R_\tau = 1343$  (dark blue), 1475 (green), 1616 (dark red), 1779 (yellow), 1962 (purple), 2088 (light blue) and 2571 (light red) compared with the universal velocity profile using (a) optimal parameters from table 4, (b) average parameters from 1. Profiles are separated vertically by 10 units.

Average parameter values are used for each profile on the right.

$$(\bar{k}, \bar{a}, \bar{m}, \bar{b}, \bar{n}) = (0.4233, 24.9583, 1.1473, 0.1752, 2.1707)$$

ZPG Turbulent Boundary Layer experimental data,  $R_\tau = 2109$  to  $17207$ 

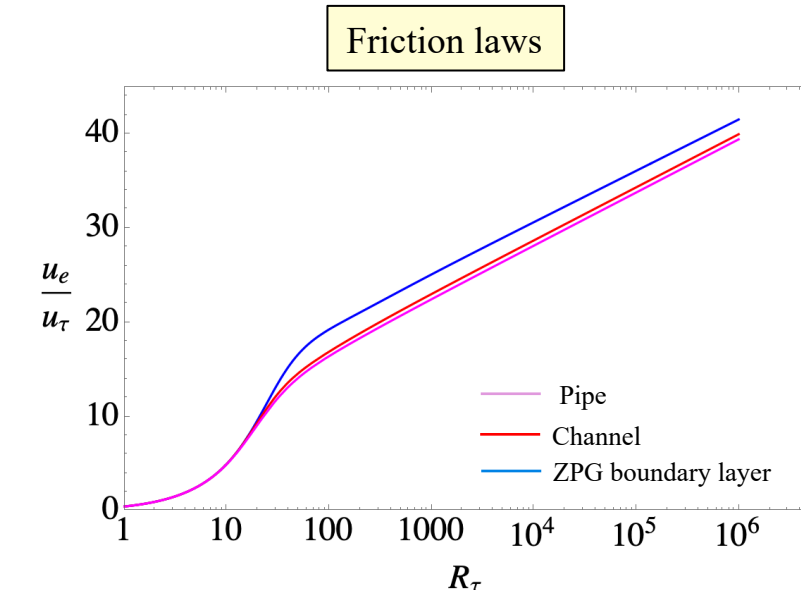
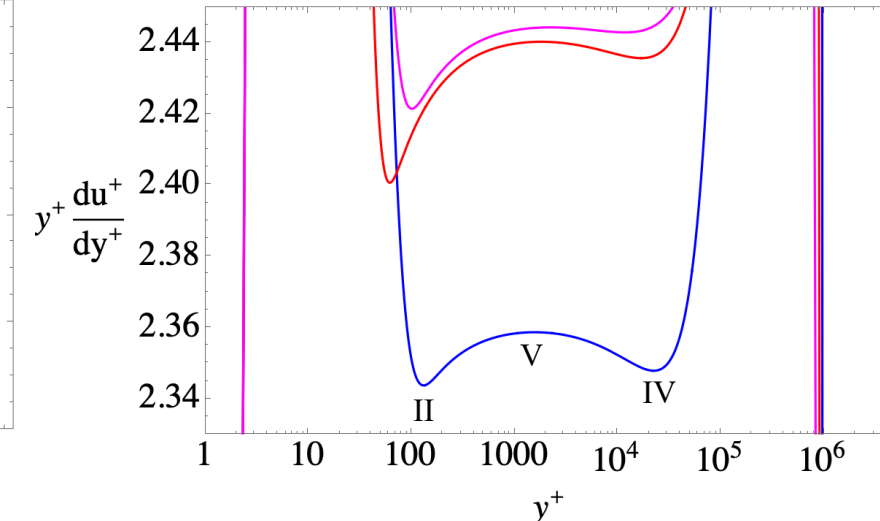
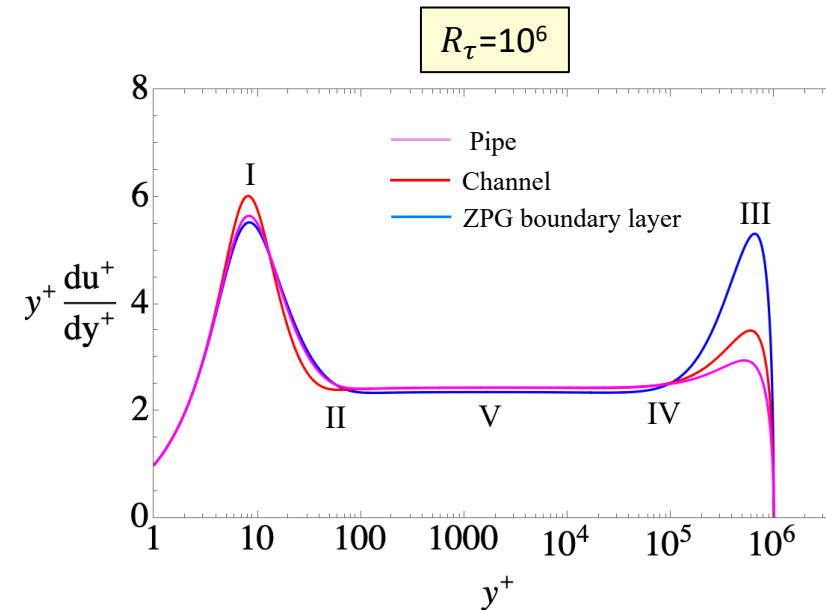
R. Baidya, J. Phillip, N. Hutchins, J.P. Monty & I. Marusic 2021 Spanwise velocity statistics in high-Reynolds-number turbulent boundary layers. *J. Fluid Mech.* 913, A35.

## Average parameter values for pipe, channel and ZPG boundary layer flows

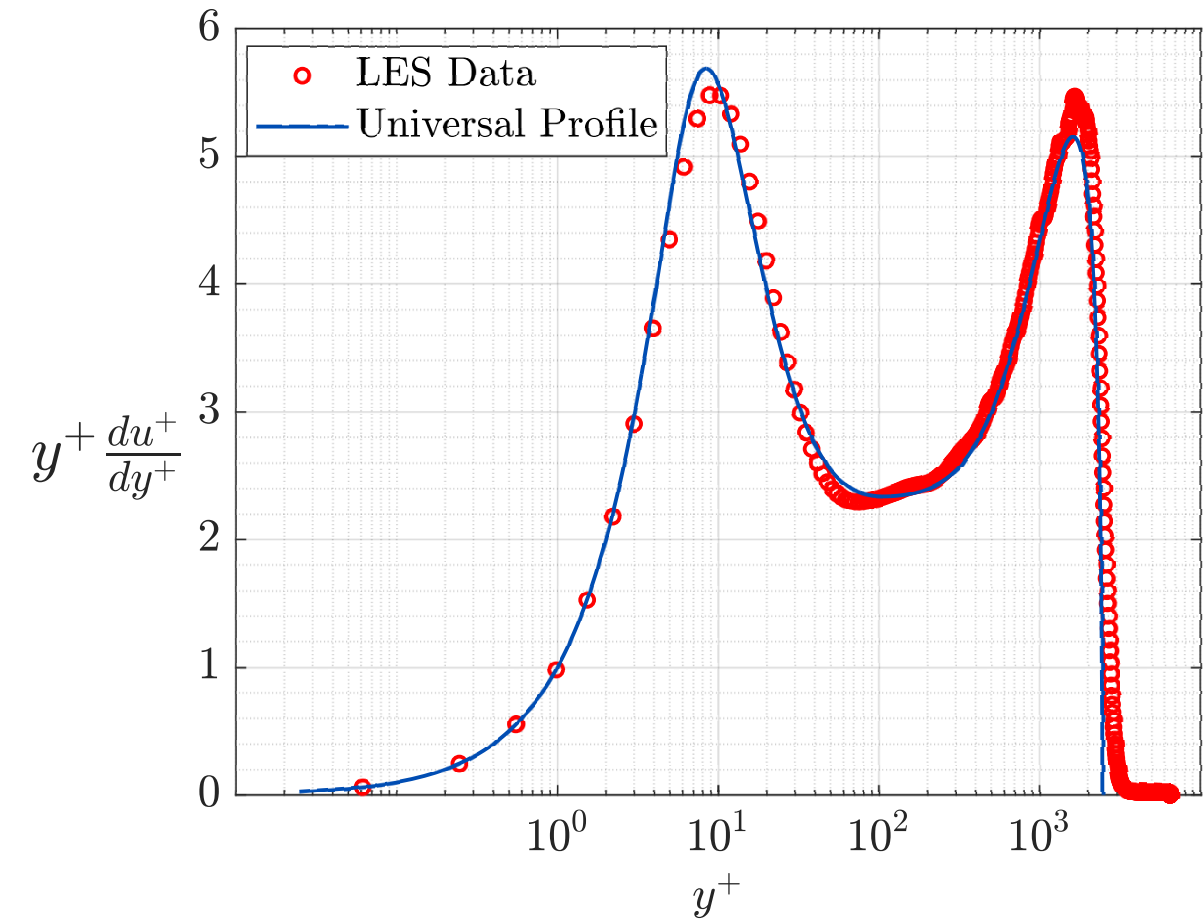
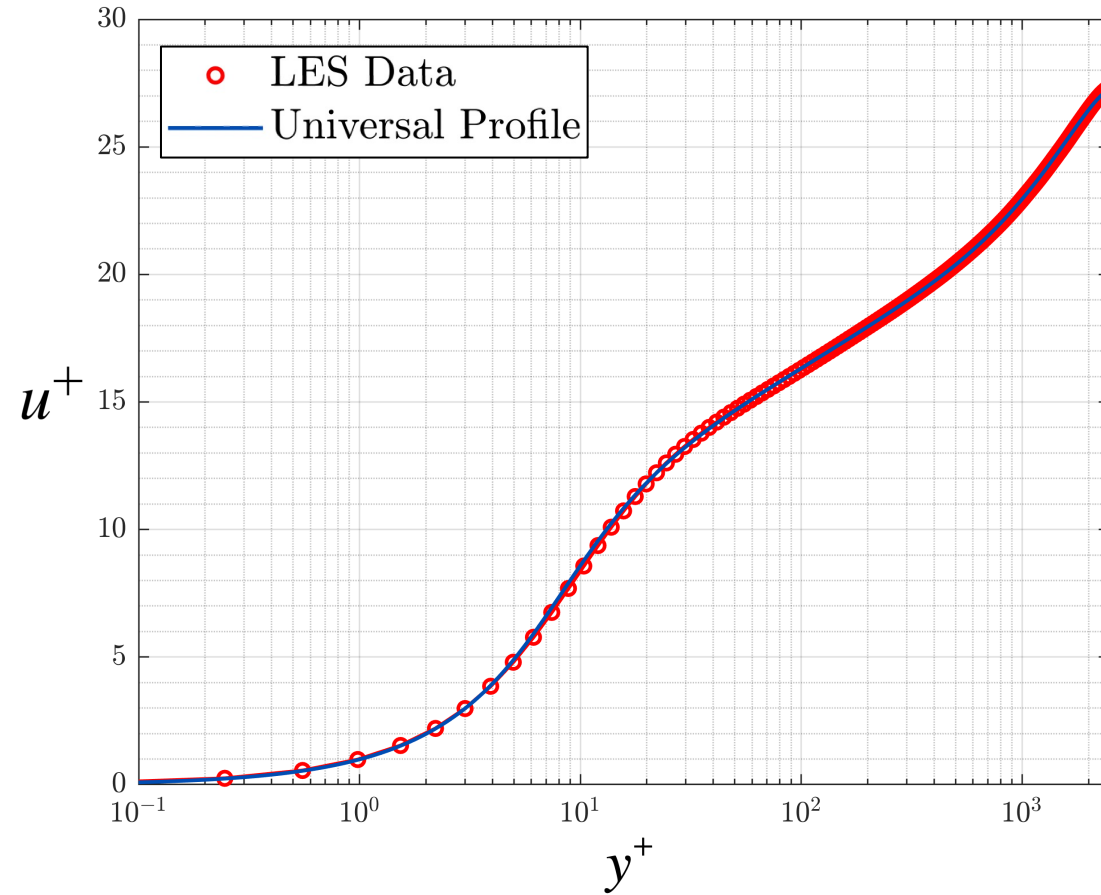
**TABLE I.** Average model parameters with standard deviation for basic wall flows. Ranges of  $R_\tau$  for each flow are as follows: Pipe (3327–530 023), Channel (550–8016), ZPG boundary layer (1343–17 207).

Flow	$\bar{k}$	$\sigma_k$	$\bar{a}$	$\sigma_a$	$\bar{m}$	$\sigma_m$	$\bar{b}$	$\sigma_b$	$\bar{n}$	$\sigma_n$
Pipe (21 profiles)	0.4092	0.0057	20.0950	0.381	1.6210	0.0379	0.3195	0.0157	1.6190	0.1204
Channel (7 profiles)	0.4086	0.0179	22.8673	1.599	1.2569	0.0292	0.4649	0.0485	1.3972	0.1213
ZPG boundary layer (11 profiles)	0.4233	0.0068	24.9583	0.663	1.1473	0.0373	0.1752	0.0060	2.1707	0.2238

## Landmarks in the log indicator function of the UVP at high Reynolds number



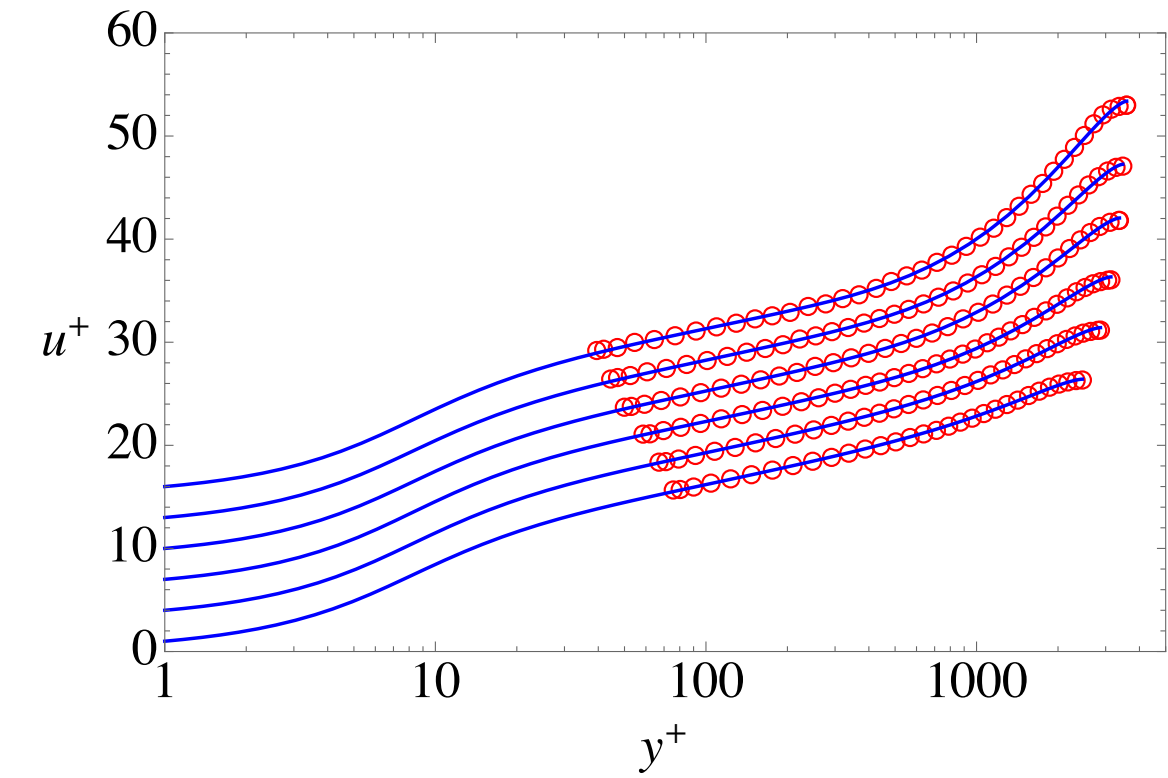
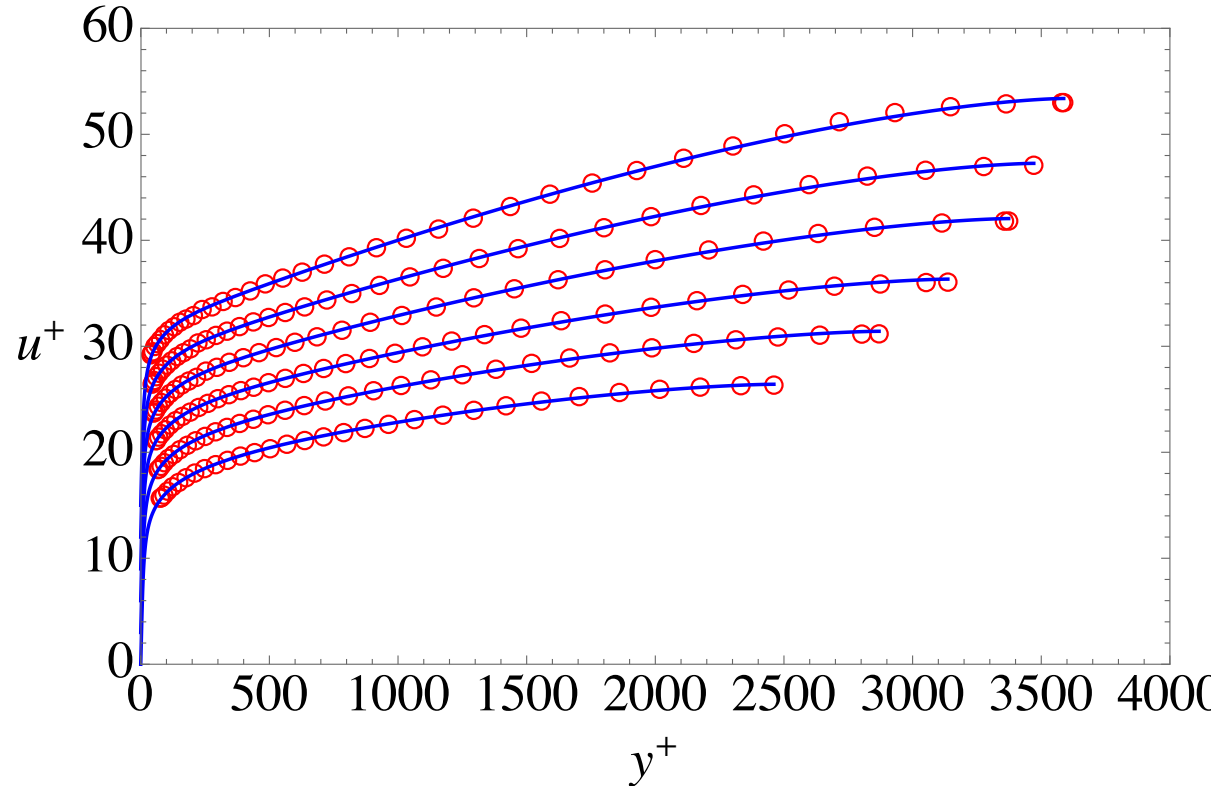
Flow	$(y^+)_I$	$(y^+)_II$	$(y/\delta_h)_{III}$	$(y/\delta_h)_{IV}$
Pipe	8.1214	62.057	0.5942	0.01698
Channel	8.2527	101.540	0.5182	0.01181
ZPG boundary layer	8.3155	132.137	0.6576	0.02557

UVP fit to Turbulent Boundary Layer LES  
simulation data  $R_\tau = 2571$ .

G. Eitel-Amor, R. Örlu and P. Schlatter, Simulation and validation of a spatially evolving turbulent boundary layer up to  $Re_\theta = 8300$ . *Intl J. Heat Fluid Flow* 47, 57–69 2014 .

## Turbulent Boundary Layer Flow with pressure gradient

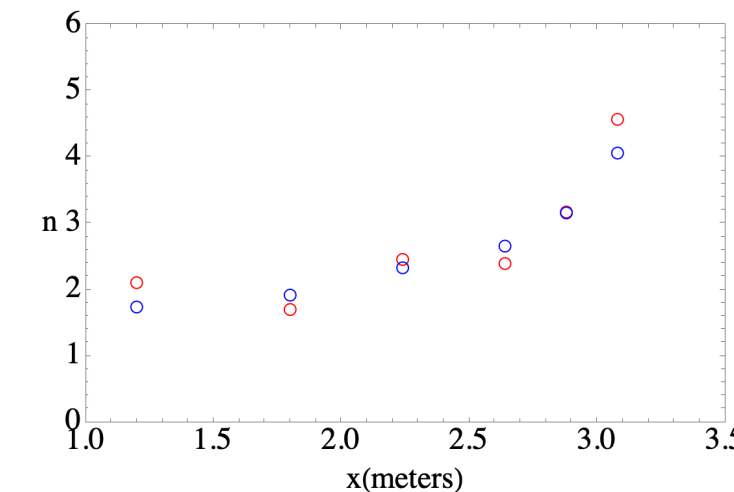
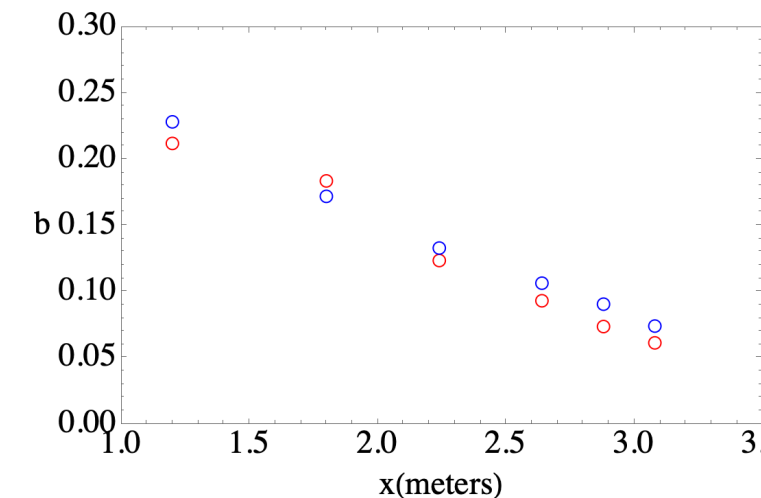
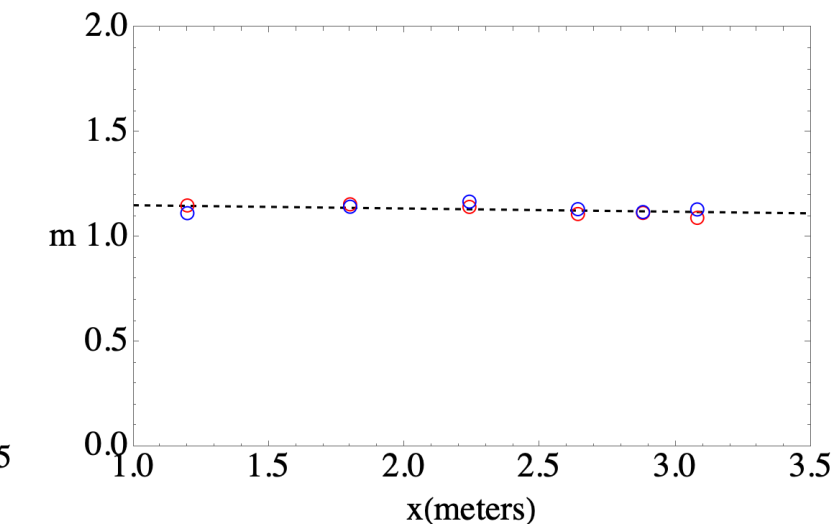
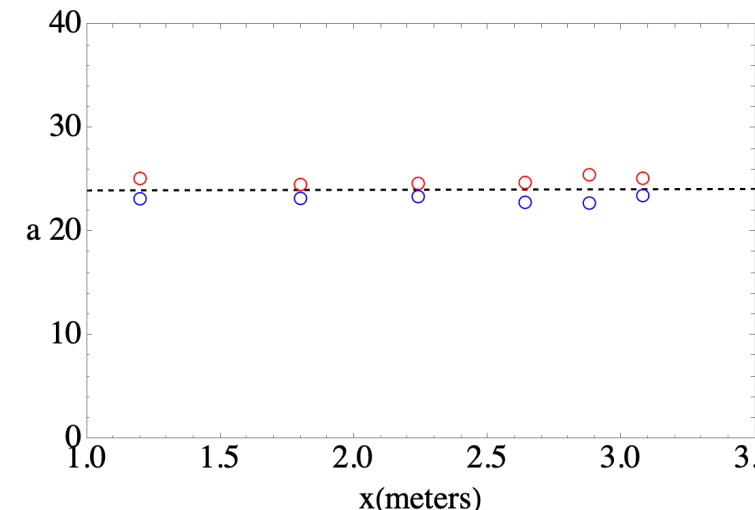
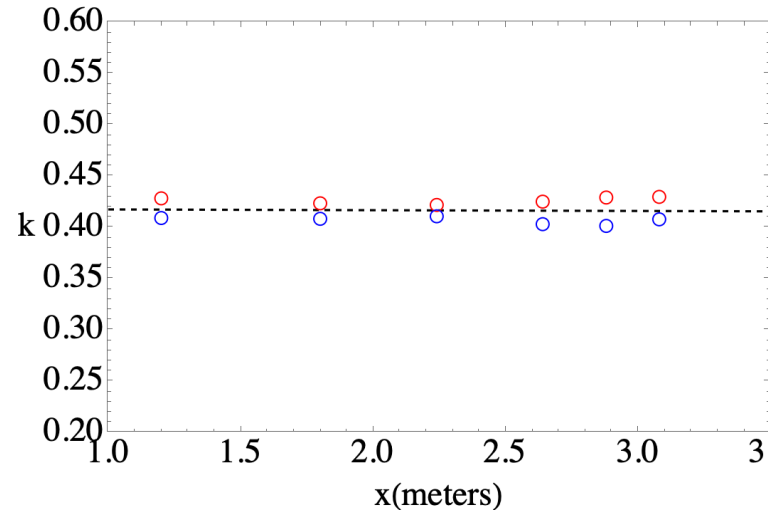
## Adverse pressure gradient Turbulent Boundary Layer experimental data, $R_\tau = 2461$ to $3587$



Perry, A.E. & Marusic, I. 1995 A wall-wake model for the turbulence structure of boundary layers. Part 1. Extension of the attached eddy hypothesis. *J. Fluid Mech.* 298, 361–388.

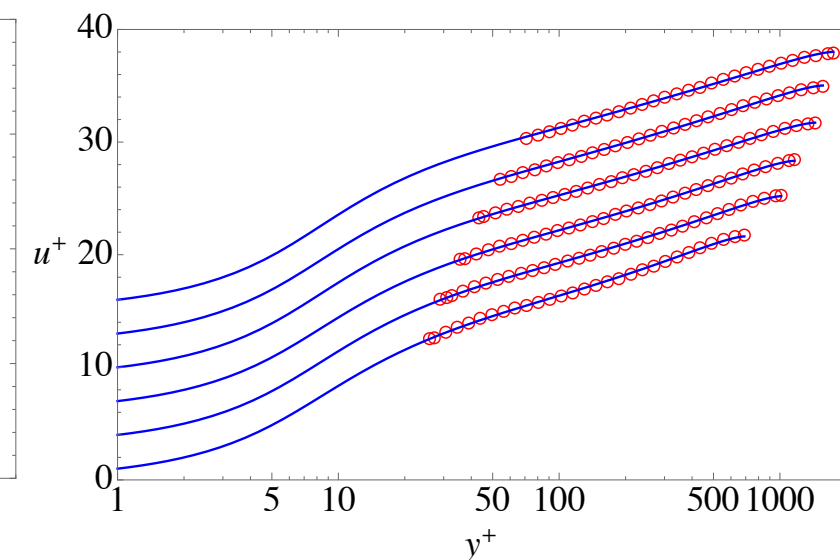
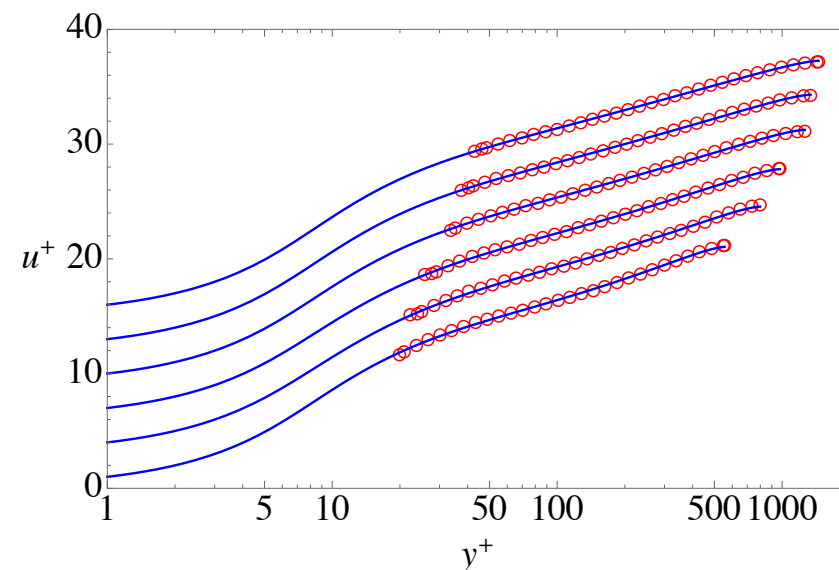
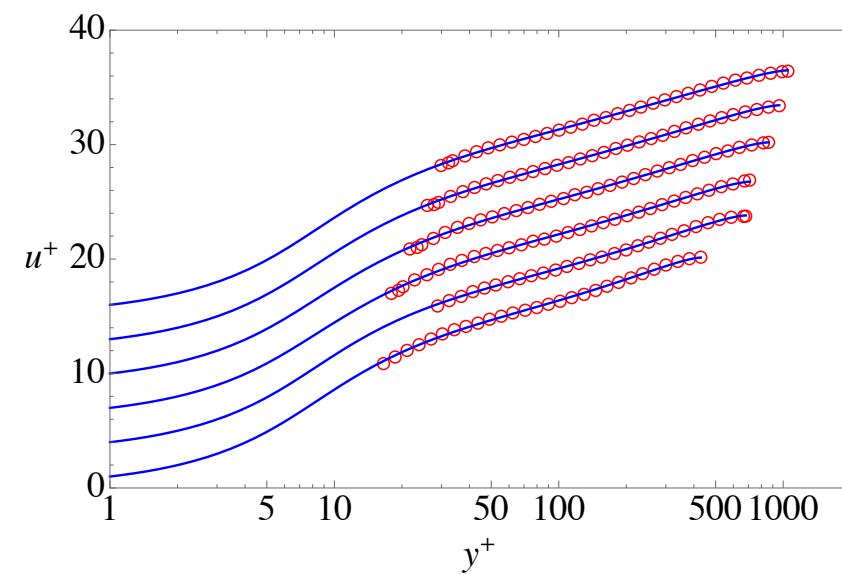
Average rms error =  
0.148, ~ 0.46%  
 $\delta_h = \delta_{0.998}$

*Changes in boundary layer wall parameters ( $k$ ,  $a$ ,  $m$ ) in an adverse pressure gradient are small.*



$\circ$   $u_\infty = 10$  m/sec  
 $\circ$   $u_\infty = 30$  m/sec

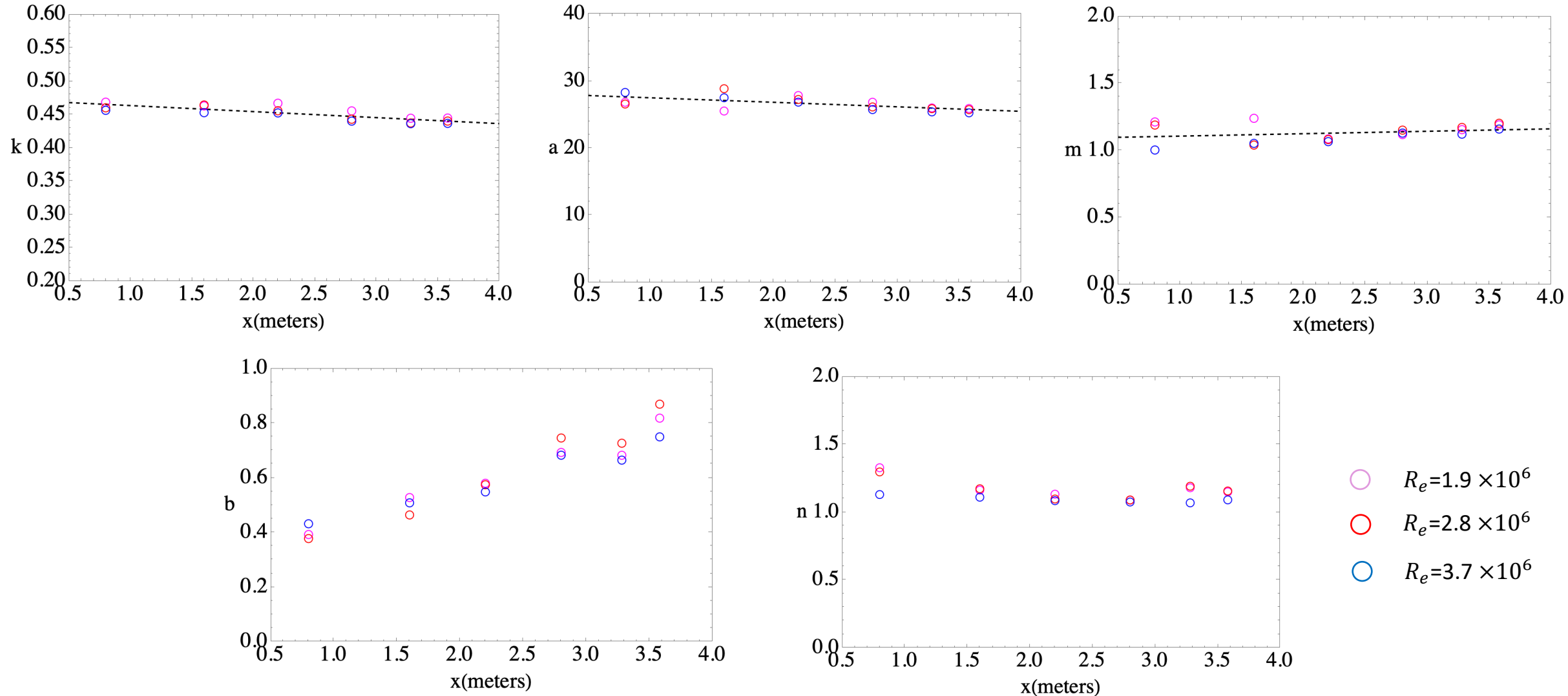
Favorable pressure gradient Turbulent Boundary Layer experimental data,  $R_\tau = 429$  to  $1746$ .



M. Jones, I. Marusic, and A. E. Perry, "Evolution and structure of sink-flow turbulent boundary layers," Journal of Fluid Mechanics 428, 1 – 27 (2001).

Average rms error  
 $= 0.075, \sim 0.36\%$   
 $\delta_h = \delta_{0.996}$

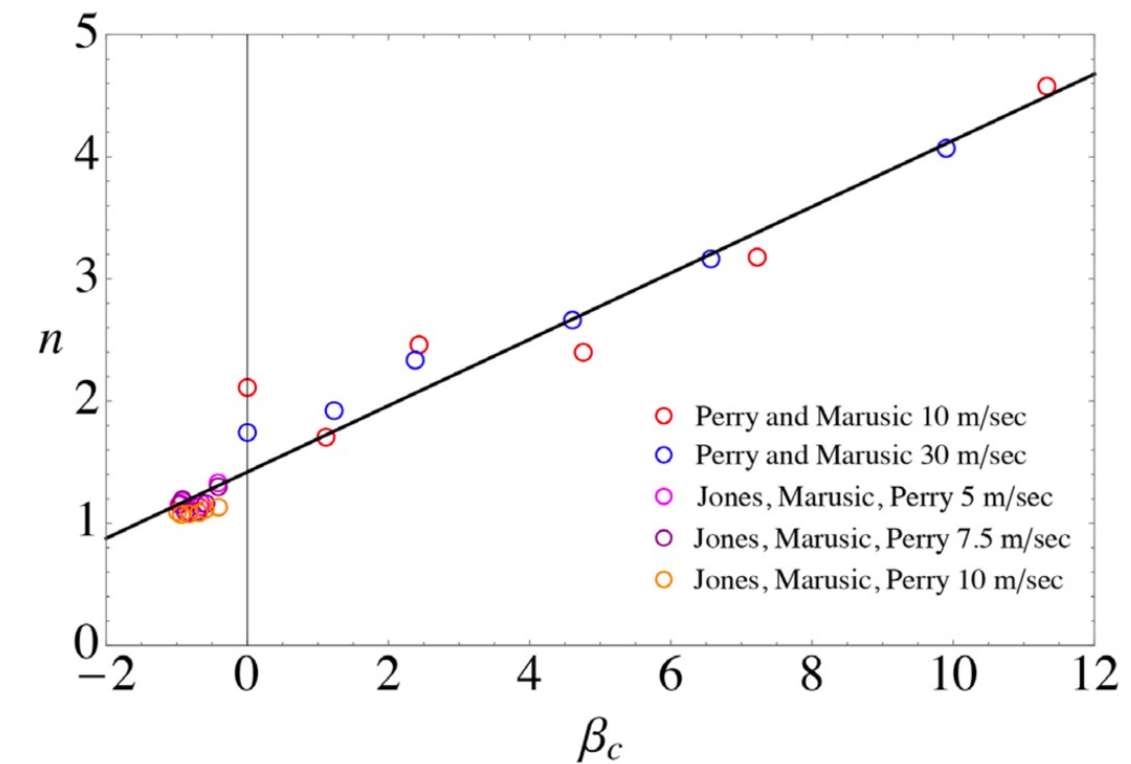
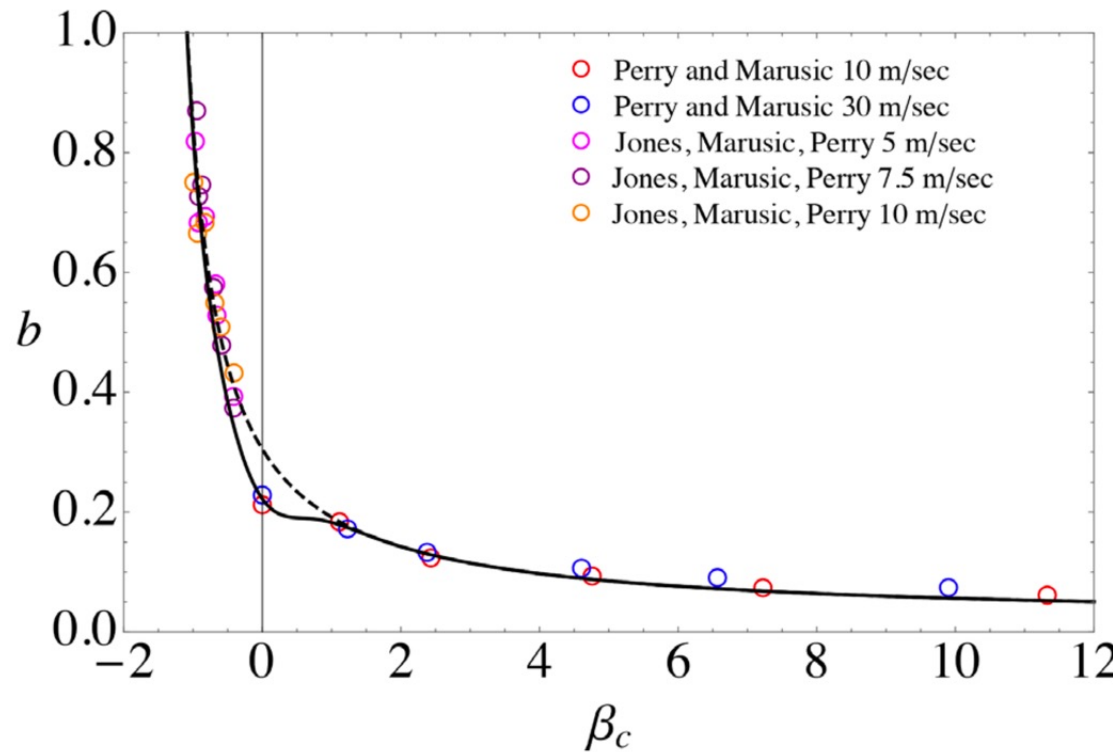
*Changes in boundary layer wall parameters ( $k$ ,  $a$ ,  $m$ ) in a favorable pressure gradient are relatively small.*



Define a modified Clauser pressure gradient parameter.

$$\beta_c = \frac{\delta_1 + \delta_2}{\tau_w} \frac{dp_e}{dx}$$

UVP wake parameters  $b$  and  $n$  are related through  $\beta_c$



## High Reynolds number

## Recall the UVP

$$u^+(k, a, m, b, n, R_\tau, y^+) = \int_0^{y^+} \frac{2\left(1 - \frac{s}{R_\tau}\right)}{1 + \left(1 + 4\lambda^2\left(1 - \frac{s}{R_\tau}\right)\right)^{1/2}} ds$$

$$\lambda(k, a, m, b, n, R_\tau, y^+) = \frac{ky^+(1 - e^{-(y^+/a)^m})}{\left(1 + \left(\frac{y^+}{bR_\tau}\right)^n\right)^{1/n}}$$

Carry out a scaling - Multiply and divide the damping and wake terms by  $k$

Modified wall-wake mixing length function.  
The parameters  $k$  and  $a$  become one parameter  $ka$ .

$$\lambda(k, a, m, b, n, R_\tau, y^+) = \frac{ky^+(1 - e^{-(y^+/a)^m})}{\left(1 + \left(\frac{y^+}{bR_\tau}\right)^n\right)^{1/n}} = \frac{ky^+(1 - e^{-(ky^+/ka)^m})}{\left(1 + \left(\frac{ky^+}{bR_\tau}\right)^n\right)^{1/n}} = \tilde{\lambda}(ka, m, b, n, kR_\tau, ky^+)$$

$$y^+ \rightarrow ky^+$$

$$R_\tau \rightarrow kR_\tau$$

Scaled velocity profile

$$ku^+(ka, m, b, n, kR_\tau, ky^+) = \int_0^{ky^+} \frac{2\left(1 - \frac{s}{kR_\tau}\right)}{1 + \left(1 + 4\tilde{\lambda}^2\left(1 - \frac{s}{kR_\tau}\right)\right)^{1/2}} ds$$

$$u/u_\tau \rightarrow ku/u_\tau$$

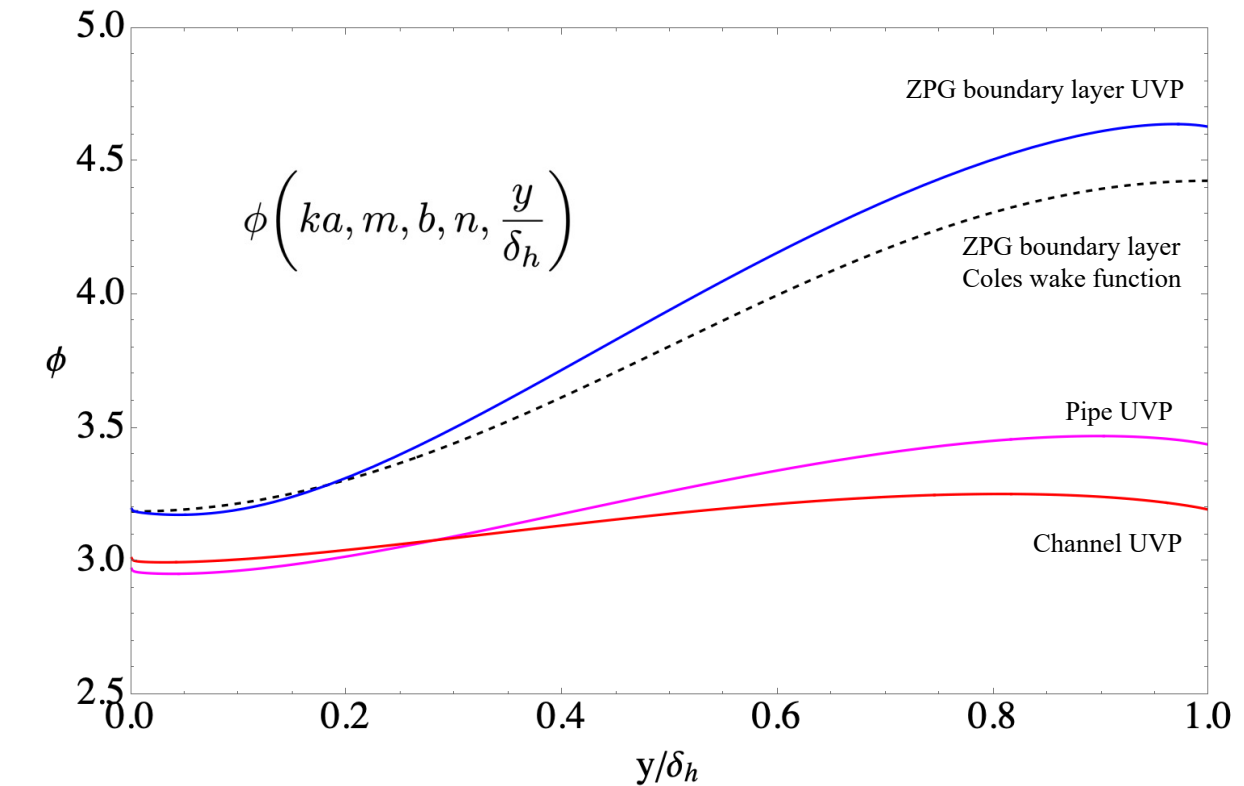
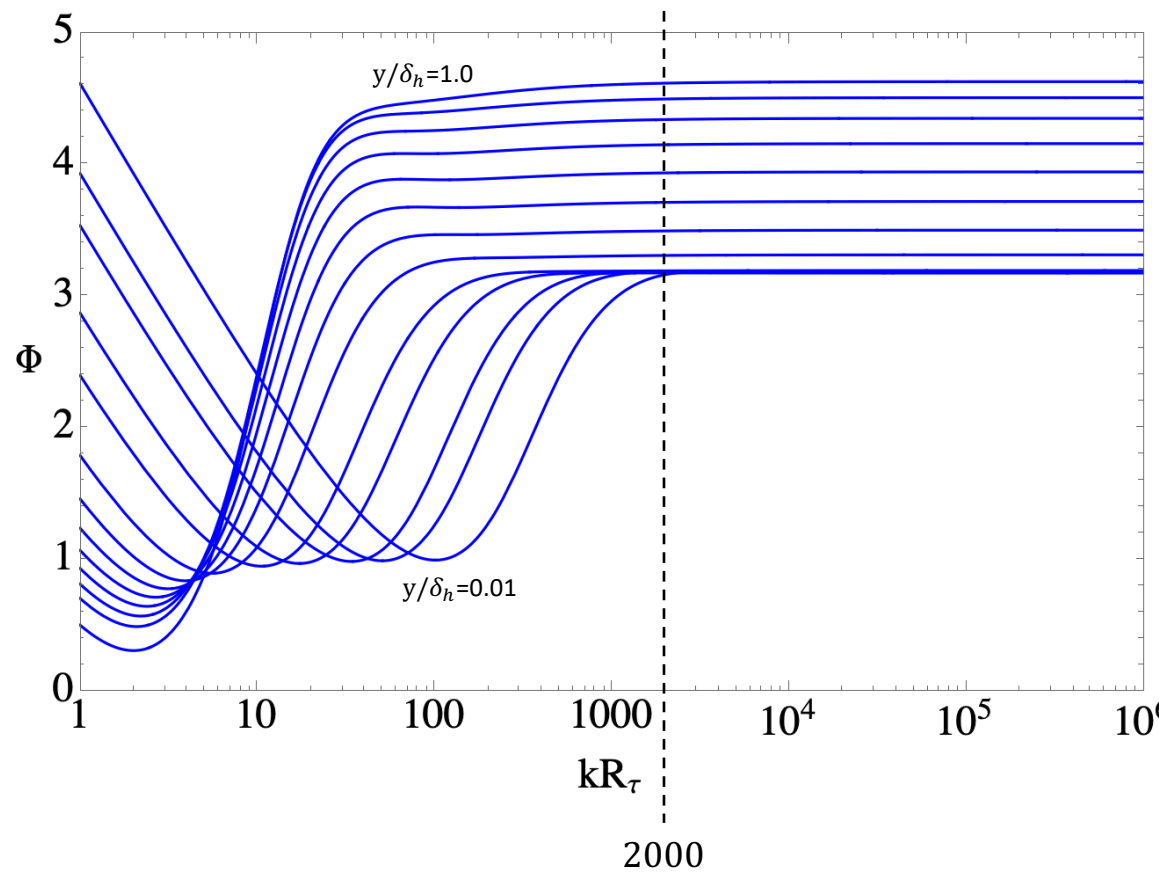
## Define the shape function

$$\Phi(ka, m, b, n, kR_\tau, ky^+) = \int_0^{ky^+} \frac{2\left(1 - \frac{s}{kR_\tau}\right)}{1 + \left(1 + 4\tilde{\lambda}^2\left(1 - \frac{s}{kR_\tau}\right)\right)^{1/2}} ds - \ln(ky^+)$$

Note       $ky^+ = \left(\frac{y}{\delta_h}\right)kR_\tau$

Fix  $y/\delta_h$  and plot  $\Phi$  versus  $kR_\tau$

Above  $kR_\tau \cong 2000$ ,  $\Phi$  is independent of  $R_\tau$



## Explicit high Reynolds number form of the UVP

At Reynolds numbers larger than  $kR_\tau \cong 2000$  the boundary layer velocity profile above  $y^+ = 132$  is accurately approximated by

$$u^+ = \frac{1}{k} \ln(ky^+) + \frac{1}{k} \phi\left(ka, m, b, n, \frac{y}{\delta_h}\right)$$

Evaluate at the boundary layer edge to determine the friction law.

$$\frac{u_e}{u_\tau} = \frac{1}{k} \ln(kR_\tau) + \frac{1}{k} \phi\left(ka, m, b, n, 1\right)$$

## The UVP friction law

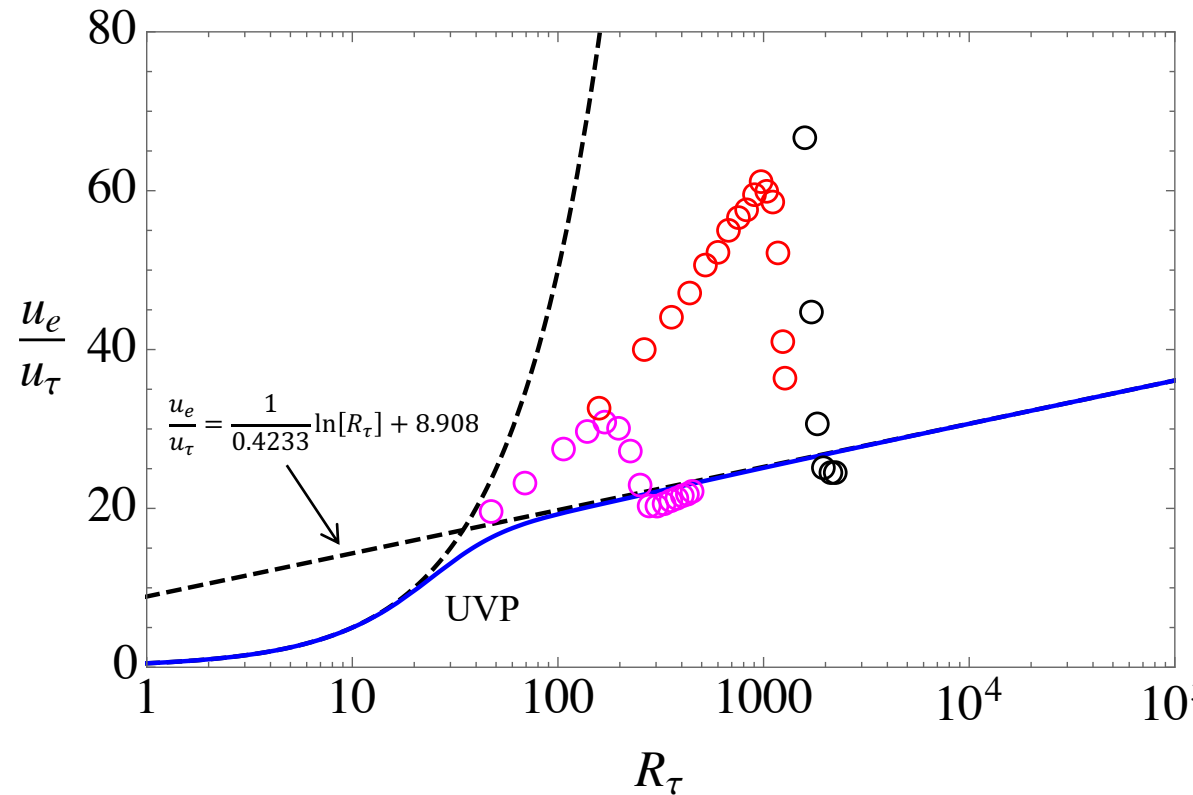


**FIG. 9.** The universal velocity profile friction law for a zero pressure gradient boundary layer along with transitional friction data from Schubauer and Klebanoff<sup>30</sup> (natural transition  $T_u = 0.03\%$ —black) and Coupland<sup>31</sup> (ERCOFTAC case T3A  $T_u = 0.9\%$ —red, case T3A  $T_u = 3.0\%$ —magenta).

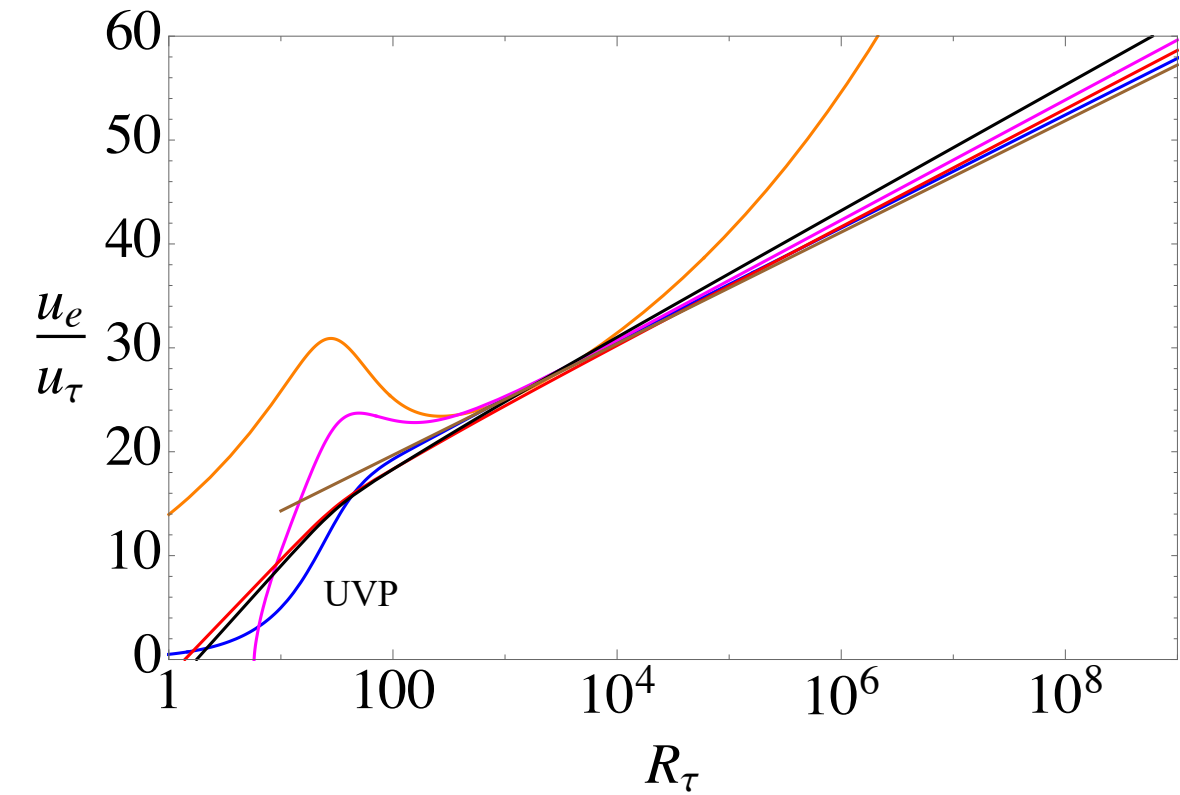
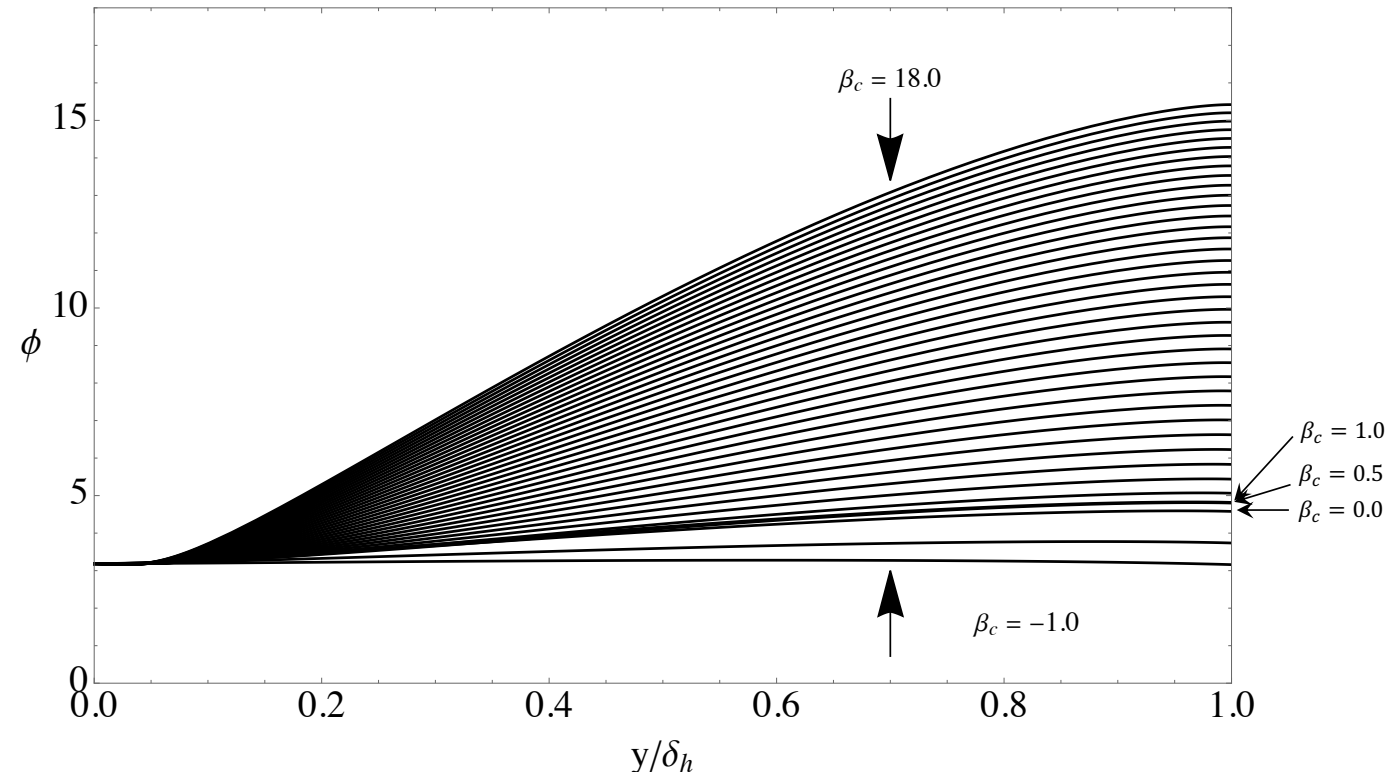


**FIG. 10.** Five friction laws compared to the UVP (blue line). The orange line is the Ludwieg-Tillman law<sup>6</sup> used in Head's method. The magenta line is the friction law developed by Nash.<sup>34</sup> The red and black lines are two versions of the Coles-Fernholz law with  $(k, C) = (0.41, 5.0)$  (red line) and  $(k, C) = (0.384, 4.1)$  (black line). The brown line is the Spalart-Allmaras law, Eq. (34), deduced from data in Polewski and Cizmas.<sup>36</sup>

## The shape function for various $\beta_c$

$$\lim_{kR_\tau > 2000} u^+ = \frac{1}{k} \ln(ky^+) + \frac{1}{k} \phi\left(ka, m, \beta_c, \frac{y}{\delta_h}\right)$$



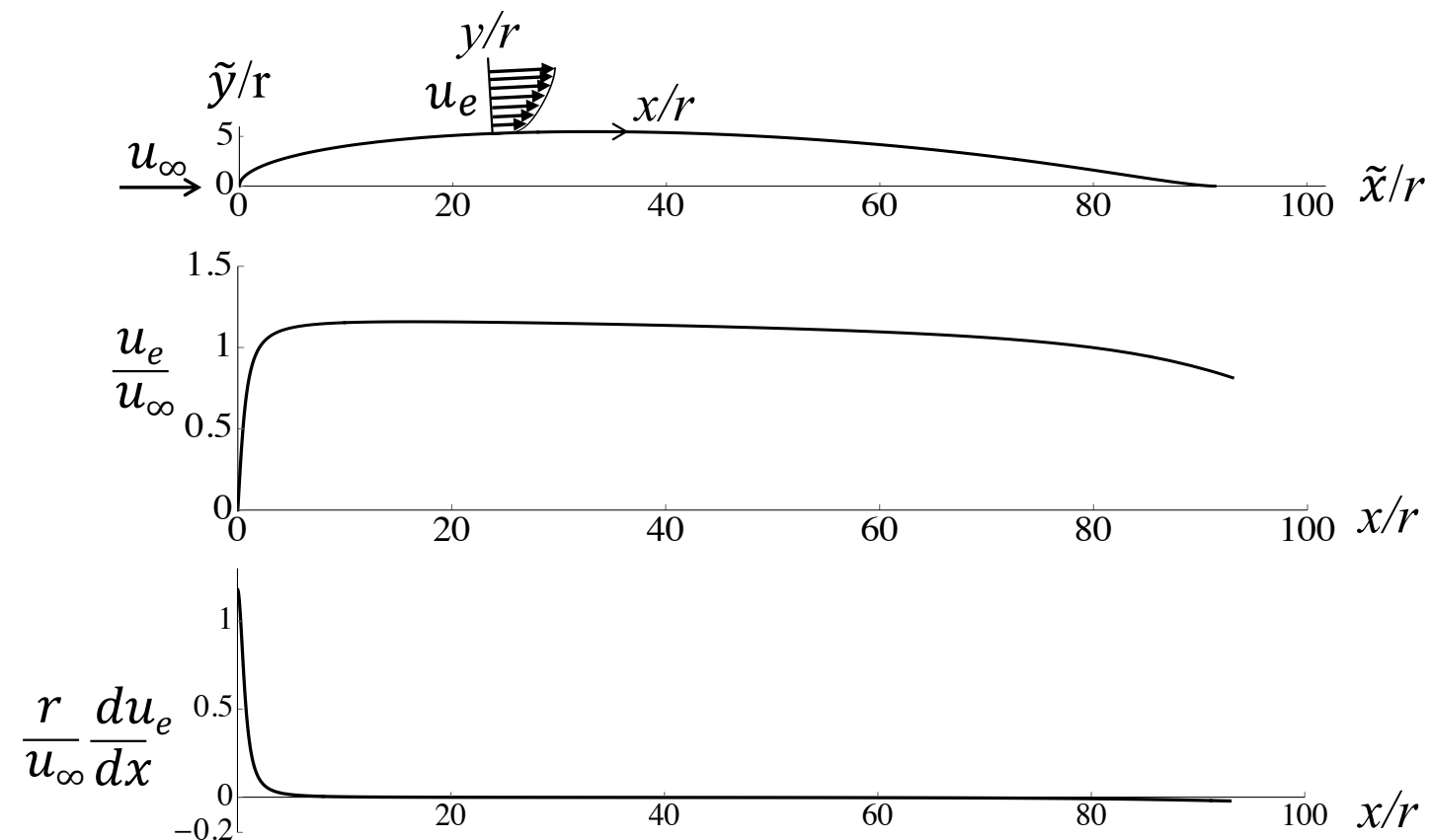
A new boundary layer integral method.

## Zero angle of attack viscous drag of Joukowsky and NACA 0012 airfoils

Choose the airfoil nose radius,  $r$ , as the characteristic length scale.  
Let  $\xi = x/r$  where  $x$  is the coordinate along the airfoil surface.

B. J. Cantwell, E. Bilgin, and J. T. Needels, "A new boundary layer integral method based on the universal velocity profile," *Physics of Fluids* 34, 075130 (2022).

Use the Hiemenz solution to approximate the stagnation point flow near the leading edge



Reynolds number based on nose radius

$$R_e = \frac{u_\infty r}{\nu}$$

From potential flow

$$\frac{u_e}{u_\infty} = U(\xi)$$

$$\xi = \frac{x}{r}$$

## Boundary layer integrals in terms of the UVP

$$R_\tau < 2000/k$$

$$u^+ = \int_0^{y^+} \frac{2\left(1 - \frac{s}{R_\tau}\right)}{1 + \left(1 + 4\lambda^2\left(1 - \frac{s}{R_\tau}\right)\right)^{1/2}} ds$$

$$\frac{u_e}{u_\tau} = \int_0^{R_\tau} \frac{2\left(1 - \frac{s}{R_\tau}\right)}{1 + \left(1 + 4\lambda^2\left(1 - \frac{s}{R_\tau}\right)\right)^{1/2}} ds \equiv F_0(R_\tau)$$

For  $R_\tau < 2000/k$ ,  $F_1, F_2$  and  $F_3$  require nested integration and can be relatively slow to evaluate especially at high Reynolds number.

$$R_\tau > 2000/k$$

$$u^+ = \frac{1}{k} \ln(ky^+) + \frac{1}{k} \phi\left(ka, m, \beta_c, \frac{y}{\delta_h}\right)$$

$$\frac{u_e}{u_\tau} = \frac{1}{k} \ln(R_\tau) + \frac{1}{k} \ln(k) + \frac{1}{k} \phi\left(ka, m, \beta_c, 1\right) \equiv F_0(R_\tau)$$

$$R_{\delta_1} = \frac{u_e \delta_1}{v} = \frac{u_e}{u_\tau} \int_0^{R_\tau} \left(1 - \frac{u_\tau}{u_e} u^+\right) dy^+ \equiv F_1(R_\tau)$$

$$R_{\delta_2} = \frac{u_e \delta_2}{v} = \int_0^{R_\tau} u^+ \left(1 - \frac{u_\tau}{u_e} u^+\right) dy^+ \equiv F_2(R_\tau)$$

$$\frac{dF_2}{dR_\tau} \equiv F_3(R_\tau)$$

For  $R_\tau > 2000/k$ ,  $F_0, F_1, F_2$  and  $F_3$  are known explicitly as algebraic and logarithmic functions of  $R_\tau$  and can be evaluated quickly at any Reynolds number.

Use the Karman integral equation to relate  $R_\tau$  to  $\xi = x/r$ .

$$\frac{d\delta_2}{dx} + (2\delta_2 + \delta_1) \frac{1}{u_e} \frac{du_e}{dx} - \left( \frac{u_\tau}{u_e} \right)^2 = 0$$

$$\beta_c = \frac{\delta_1 + \delta_2}{\tau_w} \frac{dp_e}{ds}$$

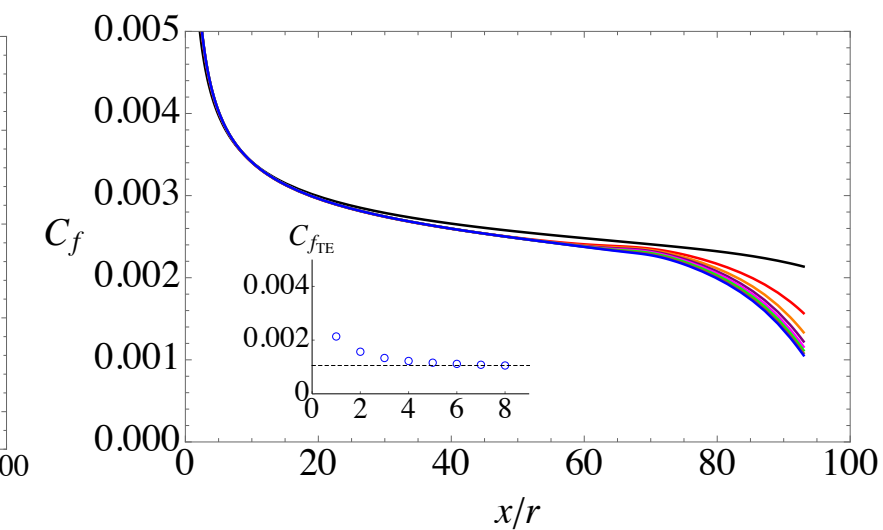
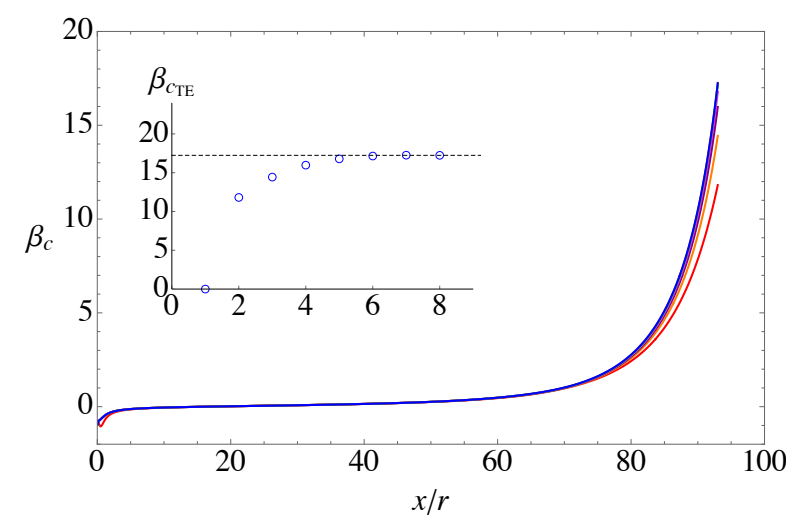
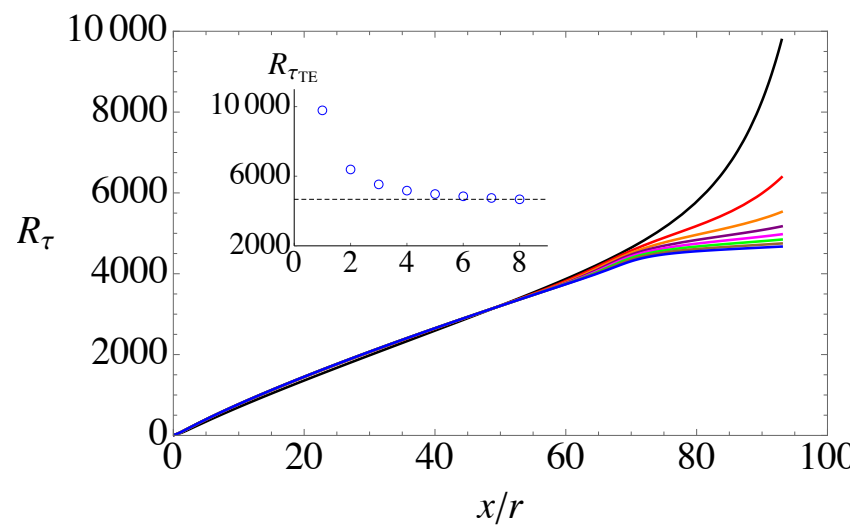
$$\frac{dR_\tau}{d\xi} = \frac{UR_e}{F_0^2 F_3} \left( 1 - \frac{F_0^2}{R_e} (F_2 + F_1) \frac{1}{U^2} \frac{dU}{d\xi} \right)$$

$$\beta_c = -\frac{F_0^2}{R_e} (F_2 + F_1) \frac{1}{U^2} \frac{dU}{d\xi}$$

Use  $\beta_c$  to adjust  $b$  and  $n$  at each streamwise point.

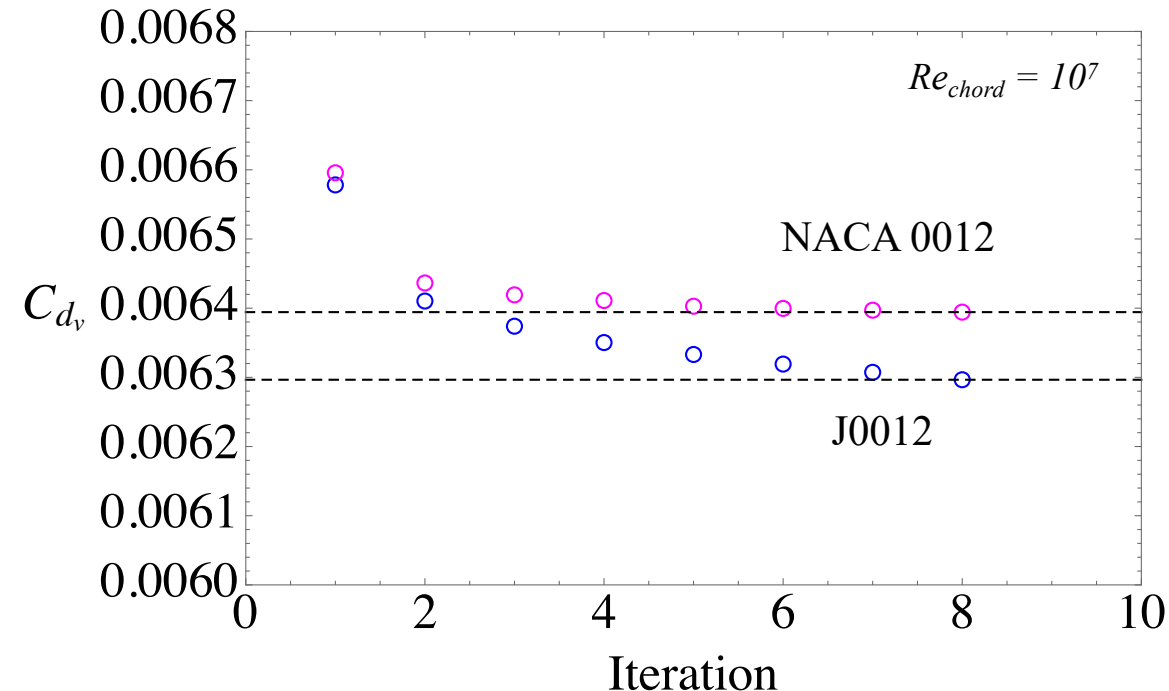
Assume the boundary layer wall parameters ( $k, a, m$ ) do not depend on the pressure gradient.

## Iterations J0012

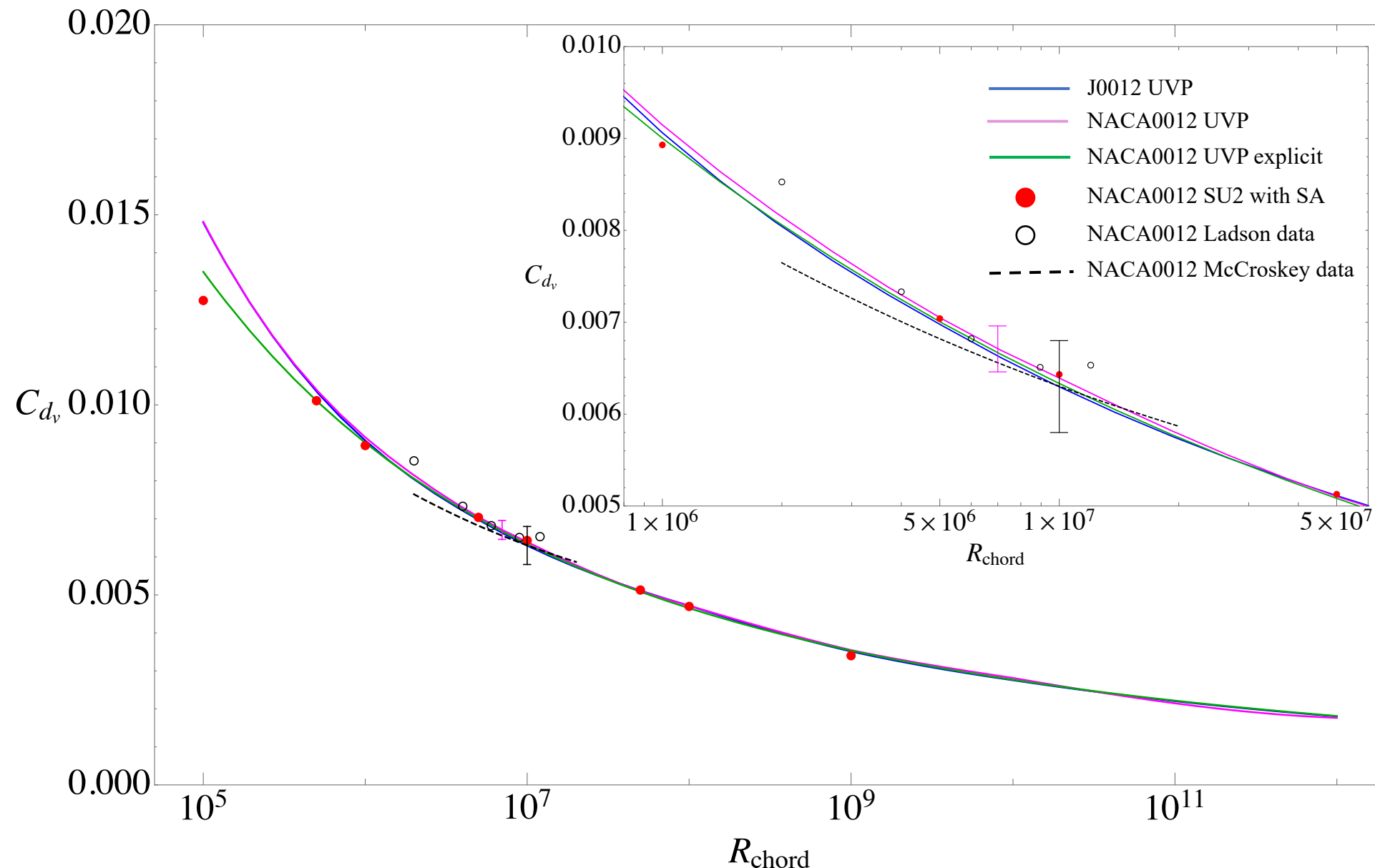
 $\text{Re}_{\text{chord}} = 10^7$ 

## Viscous drag coefficient convergence

$$C_{d_v} = \frac{D_v}{\frac{1}{2}\rho u_\infty^2 c} = 2 \int_0^1 \left( \frac{u_e}{u_\infty} \right)^2 C_f d\left(\frac{\tilde{x}}{c}\right)$$



## Main Results



## Conclusions

- 1) The UVF provides a useful replacement of the Coles wall-wake profile.
- 2) The velocity profile that accurately approximates pipe, channel and boundary layer flows is fundamentally the same function.
- 3) At Reynolds numbers larger than  $kR_\tau \cong 2000$  the UVF approaches 
$$\lim_{kR_\tau > 2000} u^+ = \frac{1}{k} \ln(ky^+) + \frac{1}{k} \phi\left(ka, m, \beta_c, \frac{y}{\delta_h}\right)$$
 above the buffer layer.
- 4) The inherent dependence of the UVF on Reynolds number, extended to include the effect of pressure gradient, enables it to be used as the basis of a new method for integrating the Karman equation for a wide variety of attached, wall bounded flows.
- 5) There is no limit to the Reynolds number that can be computed using the UVF suggesting that, with the incorporation of an appropriate roughness model, it can be applied to very large scale aerodynamic, hydrodynamic and geophysical flows.

## The future?

Ultimately fundamental questions about the optimal parameters will need to be answered as to their numerical values, their dependence on flow geometry and their possible weak dependence on Reynolds number, free stream turbulence, surface roughness, Mach number and so forth.

*It is not clear when the high Reynolds number data required to address these questions will become available.*

Thanks to my PhD Student colleagues!



Matt Subrahmanyam  
Stanford AA



Eylul Bilgin  
Stanford AA

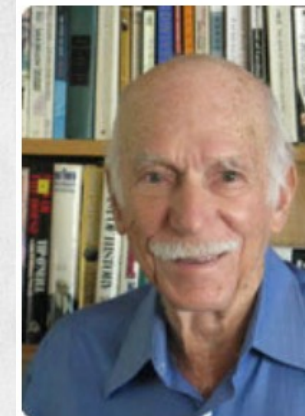


Veronika Korneyeva  
Stanford AA

## Frank Malina – Texas A&M '34



Marjorie & Frank Malina and Eileen & Martin Summerfield - Paris 1959



### David Altman

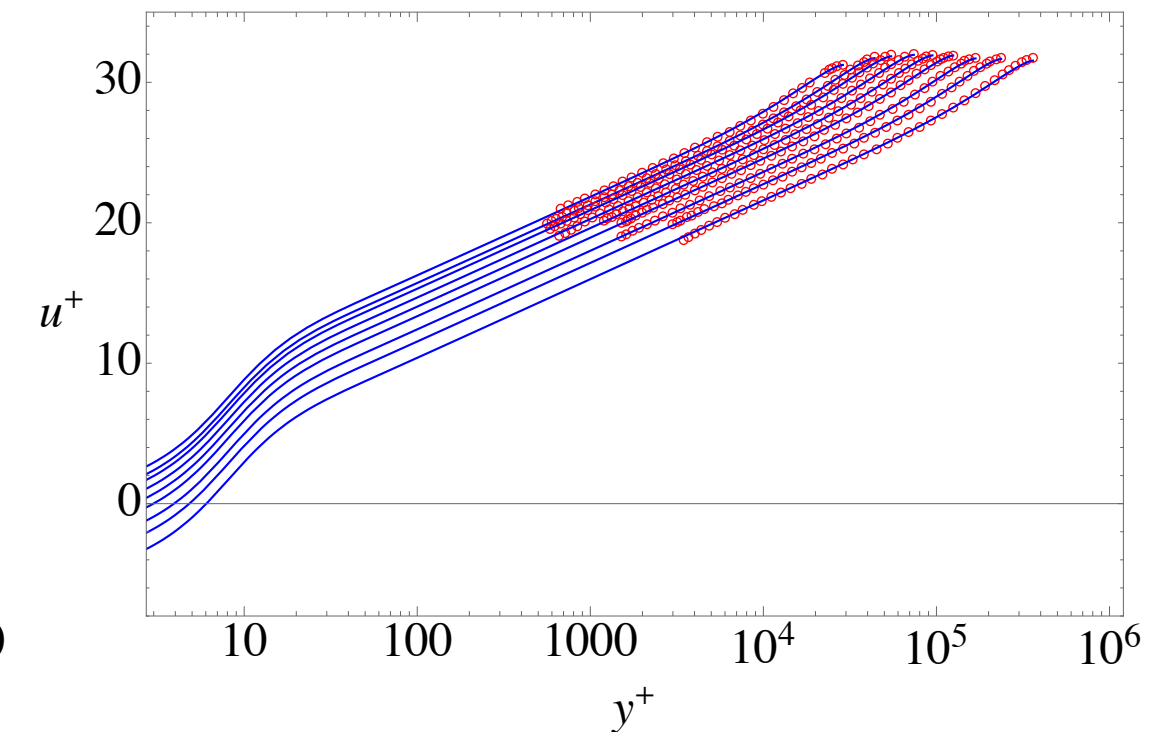
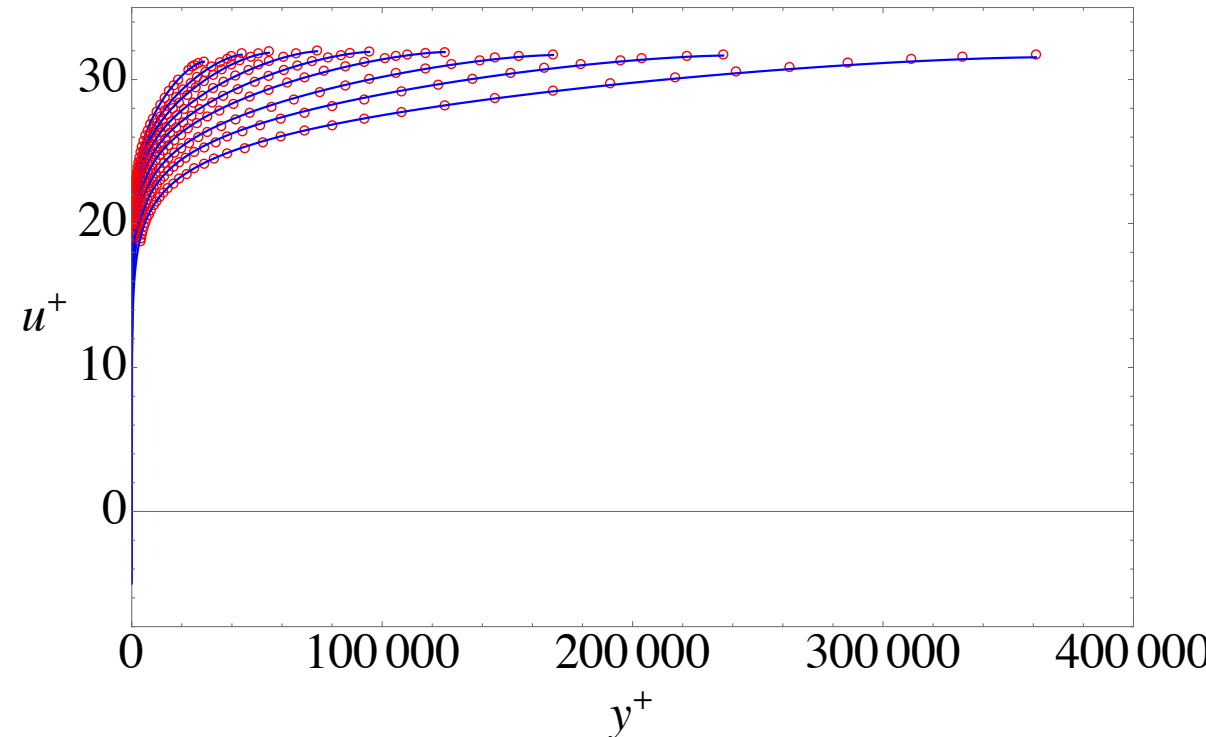
Dr. Altman's specialty is in propulsion R&D, encompassing solid, liquid, hybrid and ramjet systems. He has served on many government committees, received the AIAA Propulsion Award in 1964, the Apollo Achievement Award in 1968. He has authored numerous articles in various scientific publications including a current chapter on hybrid rockets in the 2001 Edition of the Encyclopedia of Physical Science and Technology. In 1959, Dr. Altman became involved in development of large segmented solid rockets, and in 1976 received the George Mead Medal from United Technologies Corporation for "...contributions to the 100% successful performance of solid rocket boosters during 10 years of launches" (segmented Titan boosters).

Dave Altman worked for Frank Malina during the early years of JPL, was one of the founders of the Chemical Systems Division of UTC and was a member of the Rogers Commission created to investigate the Challenger disaster. Dave lives in Menlo Park next to Stanford. He turned 103 in February.



Rough-wall pipe experimental data,  $R_\tau = 28800$  to  $361000$ 

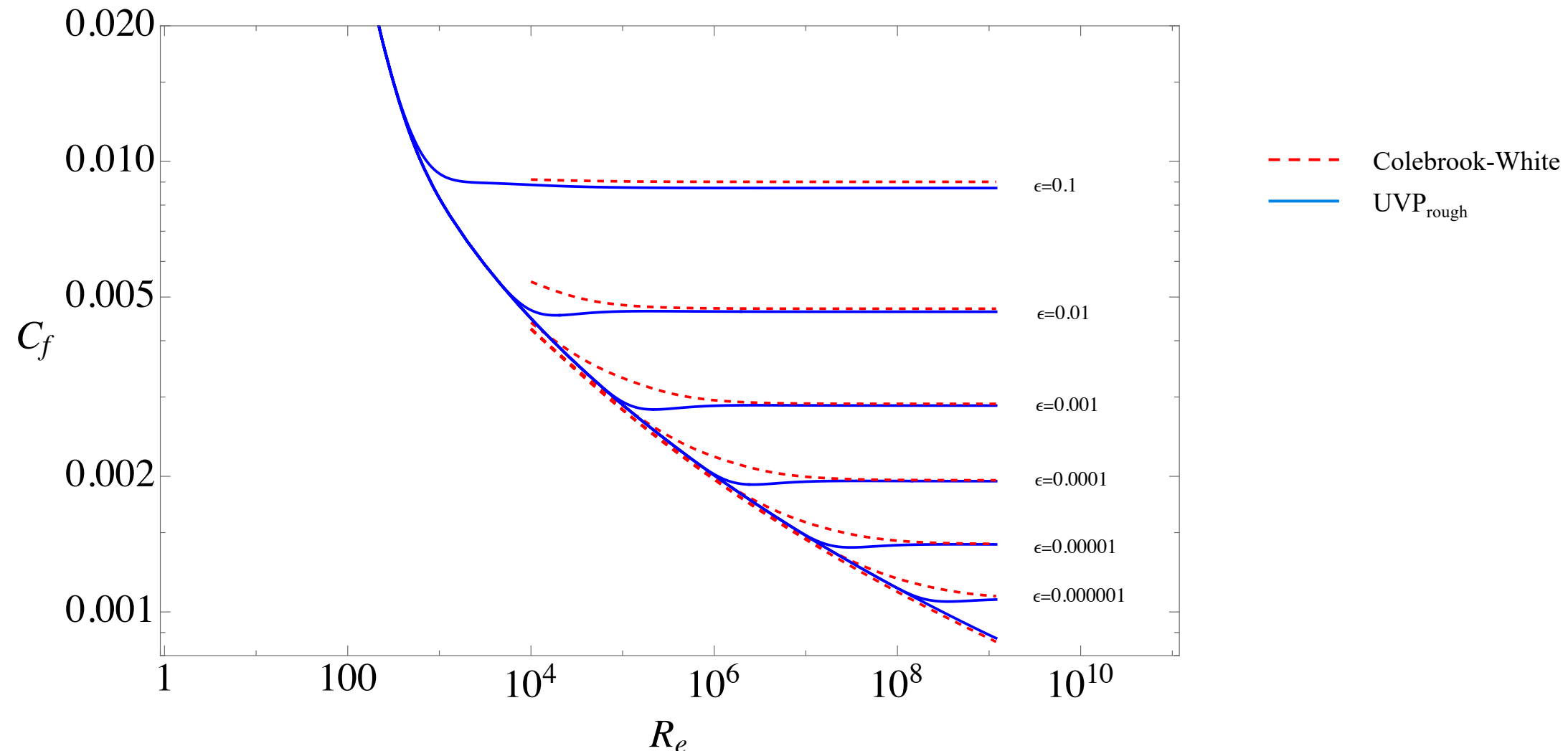
E. Bilgin and B. Cantwell, Application of the Universal Velocity Profile to rough-wall pipe flow 2023

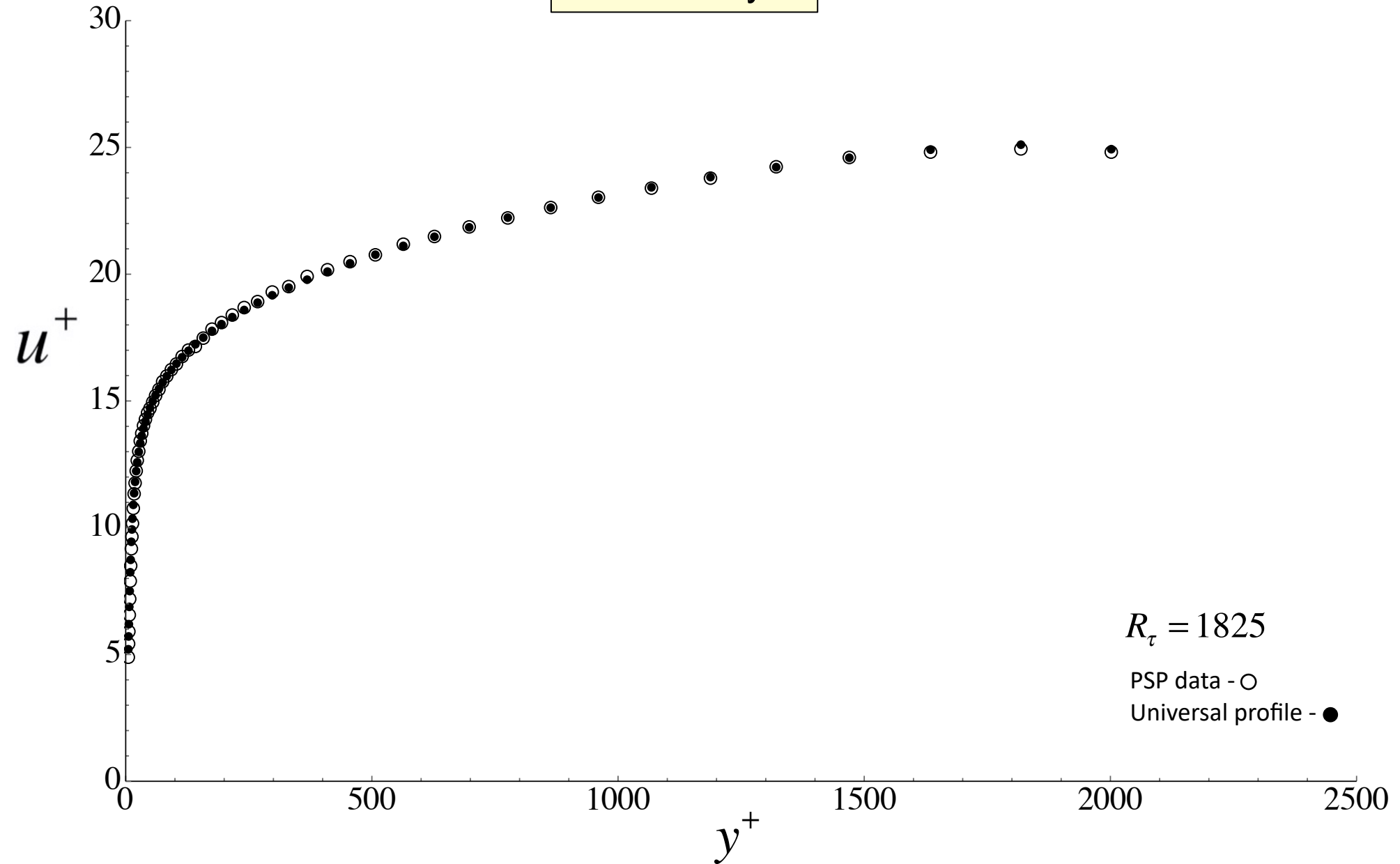


J. Allen, M. Shockling, G. Kunkel, and A. Smits, "Turbulent flow in smooth and rough pipes," Philosophical Transactions of the Royal Society A: Mathematical, Physical and Engineering Sciences 365, 699–714 (2007)

Average rms error  
 $= 0.075, \sim 0.24\%$

## Revised pipe flow Moody diagram





## Integration procedure

- 1) The first iteration uses the UVP with the constants ( $k, a, b, m, n$ ) fixed at the ZPG values ( $\beta_c = 0$ ) to determine the initial distribution of  $R_{\tau 1}(\xi)$ .
- 2)  $R_{\tau 1}(\xi)$  is then used to prepare for iteration 2. The UVP is used to compute F0, F1, F2, F3 and  $\beta_c$ . The  $\beta_c$  distribution is used determine the UVP parameters  $b(R_\tau(\xi))$  and  $n(R_\tau(\xi))$ . The wall parameters ( $k, a, m$ ) are fixed at the ZPG values. This data is used to solve for the next iteration  $R_{\tau 2}(x/r)$ .
- 3) The process is repeated until the  $i$ th iterate when  $R_{\tau i}(\xi)$  no longer changes.
- 4)  $U(\xi)$  can be updated using the airfoil+displacement thickness to recalculate the potential flow. This did not change the viscous drag measurably for the cases considered.